SYNTHESIS OF pH-SENSITIVE CHOLESTEROL POLYMERS AND *in vitro* INVESTIGATION OF INTERACTIONS WITH CELL MEMBRANE

A Thesis Submitted to
the Graduate School of Engineering and Sciences of
İzmir Institute of Technology
in Partial Fulfillment of the Requirements for the Degree of

MASTER OF SCIENCE

in Biotechnology

by
Vildan GÜVEN

July, 2014
İZMİR

We approve the thesis of **Vildan GÜVEN**

Examining Committee Members:

_____

Prof. Dr. Volga BULMUŞ
Department of Chemical Engineering, İzmir Institute of Technology

_____

Prof. Dr. Funda TIHMINLIOĞLU
Department of Chemical Engineering, İzmir Institute of Technology

_____

Assoc. Prof. Dr. Gülşah ŞANLI
Department of Chemistry, İzmir Institute of Technology

8 July 2014

_____

Prof. Dr. Volga BULMUŞ
Supervisor, Department of Chemical Engineering,
İzmir Institute of Technology

_____

Prof. Dr. Volga BULMUŞ
Head of the Department of Biotechnology
and Bioengineering

_____

Prof. Dr. R. Tuğrul SENGER
Dean of the Graduate School of
and Engineering and Sciences

ACKNOWLEDGEMENTS

Initially, I owe my deepest gratitude to all those who provided me the possibility to complete this report. A special appreciation I would like to give to my supervisor, Prof. Dr. Volga BULMUŞ, whose contribution in stimulating suggestions and encouragement, helped me to coordinate my study.

Furthermore, I am thankful to my co-workers, especially Esra AYDINLIOĞLU for her help with her endless patience and friendships throughout my study. She always listens me and cheers me. In addition, I express my thanks to my other colleagues Damla TAYKOZ, İmran ÖZER, Aykut ZELÇAK, Işıl KURTULUŞ and Ekrem ÖZER.

Moreover, I would like to acknowledge with much appreciation the friendship and support to Ender KALKAN, he always encouraged and help me whenever I want. I am also grateful to my wonderful friend, Lale ALİZADE for her emotional support. Actually she is a sister for me. What's more, I also want to thanks my other friends whose names are countless.

Special thanks are given to staff of Biotechnology and Bioengineering Research and Application Centre, Özgür YILMAZER who trained me for cell culture studies and Dane RUSÇUKLU for her help, they answer my questions whenever I need. I want to thank to Fırat ZİYANAK, Erman KIBRIS and also Doğan TAÇ.

My thanks and appreciations also go to Melda BÜYÜKÖZ and Metin UZ. They are really my guide for the intracellular distribution experiments. Additionally, I want to give my endless thank to Öznur BAŞKAN for her support with her patience in microscopy and friendship. I would like to thank to Sezen Duygu ALICI, Derya KÖSE and Melis OLÇUM as well.

The financial support of The Scientific and Technological Research Council of Turkey (through the grant# 111T960) is gratefully acknowledged.

Last but not least, the most important and special thank goes to my family. I would have not finished this project without the support of my family who has always been there for me whenever I need them, the encouragement they give to keep me going and their love to empower me that never fails all the time. Finally, I want to dedicate my thesis to my parents, Ali İhsan GÜVEN and Hamidiye GÜVEN.

ABSTRACT

SYNTHESIS OF pH-SENSITIVE CHOLESTEROL POLYMERS AND IN VITRO INVESTIGATION OF INTERACTIONS WITH CELL MEMBRANE

The aim of this thesis is to synthesize pH-sensitive, cholesterol containing polymers via reversible addition fragmentation chain transfer (RAFT) polymerization, as potential membrane-destabilizing agents for intracellular drug delivery applications and investigate interaction of these polymers with cell membrane. For this purpose, cholesteryl methacrylate (CMA) and 2-((tert-butoxycarbony)(2-((tert-butoxycarbonyl) amino) ethyl) amino)ethyl methacrylate (Boc-AEAEMA) were first synthesized. CMA was copolymerized with t-butyl methacrylate (t-BMA) or Boc-AEAEMA via RAFT polymerization to produce cholesterol containing copolymers having varying molecular weights and compositions. Copolymers were characterized using ^{1}H-NMR spectroscopy and gel permeation chromatography (GPC). Linear increase in ln $[M]_0/[M]$ with polymerization time, and Mn with monomer conversion indicated the RAFT-controlled copolymerizations under the conditions tested. P(t-BMA-co-CMA) and P(Boc-AEAEMA-co-CMA) copolymers were hydrolyzed to methacrylic acid-co-CMA (p(MAA-co-CMA) and p(AEAEMA-co-CMA) copolymers, respectively, to obtain water soluble, pH-sensitive copolymers. The pH-responsive behavior of copolymers was demonstrated via UV−visible spectroscopy and dynamic light scattering measurements. These measurements revealed that (p(MAA-co-CMA) copolymers having 2 and 4 mol% CMA form nanoparticles at pH 5.5 while they exist as unimers at pH 7.4. Copolymers having 8% CMA form aggregates at both pH values. Hemolysis assays revealed that p(MAA-co-CMA) having a molecular weight above 20,000 g/mol did not show pH-dependent hemolytic activity regardless of CMA content. The cell viability results (obtained by MTT assay) indicated that p(MAA-co-CMA) at 250 μg/ml concentration is not cytotoxic to NIH3T3 cell line.

ÖZET

pH-DUYARLI KOLESTEROL POLİMERLERİNİN SENTEZİ VE HÜCRE MEMBRANIYLA ETKİLEŞİMLERİNİN in vitro İNCELENMESİ

Bu tezin amacı, hücre içi ilaç salımı alanlarında potansiyel membran bozucu ajanlar olarak kullanılmak üzere pH-duyarlı kolesterol polimerlerinin, tersinir katılma ayrışma zincir transfer (RAFT) polimerizasyonu ile sentezlenmesi ve hücre membranıyla etkileşimlerinin *in vitro* incelenmesidir. İlk olarak kolesteril metakrilat ve (2-((tert-butoksikarbonil) (2-((tert-butoksikarbonil)amino)etil)amino) etil metakrilat monomerleri sentezlendi. Kolesteril metakrilatın, t-butil metakrilat ve (2-((tert-butoksikarbonil) (2-((tert-butoksikarbonil)amino) etil) amino) etil metakrilat ile kopolimerleri farklı moleküler ağırlıkta ve farklı kompozisyonlarda RAFT polimerizasyonu ile sentezlendi. Elde edilen polimerler, ^{1}H-NMR spektroskopisi ve jel geçirgenlik kromatografisi (GPC) ile karakterize edilmiştir. ln $[M]_0/[M]$ değerinin zaman, monomer dönüşümün ise Mn değeri ile lineer artması, RAFT kontrollü kopolimerleşme olduğunu göstermiştir. P(t-BMA-ko-CMA) ve P(Boc-AEAEMA-ko-CMA) kopolimerleri, suda çözünür ve pH-duyarlı kopolimerler elde etmek için, metakrilik asit-kolesteril metakrilat (p(MAA-ko-CMA)) ve (amino)etil)amino)etil metakrilat p(AEAEMA-ko-CMA) kopolimerlerine sırasıyla hidrolize edilmiştir. Kopolimerlerin pH'a duyarlı davranışları, UV-görünür spektroskopisi ve dinamik ışık saçılması ölçümleri ile gösterilmiştir. Bu ölçümler sayesinde, 2 mol % ve 4 mol % kolesteril metakrilat iceren pH 5.5'te (p(MAA-ko-CMA)) nanopartikül halinde pH 7.4 te ise ünimer halinde bulunmaktadırlar. 8 mol % kolesteril metakrilat içeren kopolimerler ise iki pH değerinde de agregasyon oluşturmuştur. Hemoliz deneyleri sonucu kolesterol iceriği ne olursa olsun molekül ağırlığı 20,000 g/mol'den daha yüksek p(MAA-ko-CMA) kopolimerleri pH-bağımlı hemolitik aktivite gösteremediği gözlemlenmiştir. Hücre canlılık deney sonuçları bu kopolimerlerin 250 μg/ml konsantrasyonda NIH3T3 hücre hattı için toksik özellik göstermediğini ortaya çıkarmıştır.

TABLE OF CONTENTS

APPENDICES

LIST OF FIGURES

LIST OF TABLES

Table **Page**

CHAPTER 1

INTRODUCTION

The biomacromolecular therapeutics used in gene therapy, gene silencing therapy or other such therapies cannot penetrate the plasma membrane because of their hydrophilic and macromolecular structure. The drug delivery systems play a vital role in such therapies. Particles in nanometer size and polar macromolecules use endocytosis mechanism to enter cells. In this process; cell plasma membrane extends outward and extending membrane surrounds particles. The surrounded particle in a cellular vesicle called endosome starts to deepen into the cell interior. The first compartment of endocytotic pathway is early endosome where the environment is mildly acidic. The next station is late endosome which also involves a more acidic environment. The last compartment of this pathway is lysosomes where pH is around 4.5and a variety of degradative enzymes exists. In this compartment, most substances are lysed. The therapeutic agent without a suitable delivery vehicle is entrapped in the endocytic pathway. In order to traffick the agent from the endosome; the delivery vehicle should disrupt or destabilize the endosome membrane. By this way, the therapeutic agent can be delivered to cytosol and specific intracellular organels at therapeutic concentrations. There are various viral and non-viral delivery agents that can help therapeutics to escape from endosome. Viruses and bacteria have high transfection efficiency and facilitate uptake by cells using their surface proteins. However, the safety problems such as toxicity and immunogenicity, and bulk production difficulties are their drawbacks. Although they are less efficient in escaping from endocytosis mechanism, the synthetic vectors have low toxicity and low immune response. pH-responsive polymers such as polyanions and polycations, and lipid based systems such as cationic lipids and cholesterol, are among the synthetic vectors that have been widely used in intracellular drug delivery applications. Amphiphilic polyanions can undergo from a hydrophilic, membrane-inactive state to a hydrophobic, membrane-active state by being protonated as environmental pH changes from neutral to acidic. In literature, amphiphilic polyanions have been reported to lyze cellular membranes such as endosome membrane and red blood cell membrane at acidic pHs. Such a change can be used to hydrophilicity

results in the polyanions (Henry, El-Sayed et al. 2006). The polycations are protonated at neutral or acidic pHs while they are neutral at basic pHs. Polycations, because of their positive charge, can be efficiently taken up by cells. Polycations, such as polyethylene imine, that have a number of primary, secondary and tertiary amine groups, can be protonated in a wide pH range. Such polymers can be used as proton sponges and have been shown to disrupt endosomal vesicles by efficiently buffering acidic environment. The lipid based systems such as cationic lipids and cholesterol have been efficiently used in intracellular delivery of nucleic-acid therapeutics. They are usually more efficient than polymer-based systems. However, lipid-based systems have stability and solubility problems.

In this thesis, the aim is to develop pH-responsive, cholesterol containing, well-defined polymers as potential endosomal escaping agents for intracellular drug delivery applications. For this purpose, cholesteryl methacrylate (CMA) was copolymerized with t-butyl methacrylate (t-BMA) or 2-((tert-butoxycarbony)(2-((tert-butoxycarbonyl) amino) ethyl) amino)ethyl methacrylate (Boc-AEAEMA) to produce cholesterol containing pH-responsive copolymers having varying molecular weights and compositions. To have control over the molecular weight of polymers, a living/controlled radical polymerization technique, reversible addition fragmentation chain transfer (RAFT) polymerization technique was used. The physicochemical characteristics and pH-responsive behaviors of copolymers were characterized by a variety of techniques. The in vitro cytotoxicity of copolymers was determined. The ability of copolymers to interact with cellular membranes was identified by investigating the hemolytic activity and intracellular distribution of copolymers.

CHAPTER 2

LITERATURE REVIEW

2.1. Intracellular Drug Delivery

Intracellular delivery of pharmaceutical molecules is an important challenge in drug delivery field. Several therapeutic agents should be delivered intracellularly at therapeutic concentrations to perform their therapeutic duty. The intracellular sites may include certain organelles for instance lysosomes for therapy of some lysosomal storage diseases, nuclei for delivery of DNA therapeutics, certain immunotherapeutics, protein vaccines and mitochondria for the treatment of cancer with proapoptotic anticancer drugs or inside cytoplasm for delivery of gene silencing therapeutics such as siRNA (Torchilin 2008). There are a series of barriers to systemic delivery of therapeutics such as enzymatic attacks, tightly packed endothelial cells preventing diffusion, non-specific binding to serum proteins), non-specific plasma or vessel protein interaction, activation of immune system cells, non-specific distribution, and impermeability of cell membrane to macromolecular structures Figure 2.1 (McCrudden and McCarthy 2013). Cell membrane is the most obstructive barrier to macromolecular therapeutics because of its impermeable character to large or polar molecules. The uptake of particles with large hydrodynamic volume by eukaryotic cells depends on size, charge, shape, surface chemistry, surface topology and mechanical properties (Canton and Battaglia 2012). While passive diffusion described by Fick's law is not effective in the uptake of large hydrodynamic volume molecules and particles, varying active transport mechanisms are favored for these particles. For solid-lipid nonaparticles, non-energy dependent pathway is useful because of chemical and structural likeness between plasma membrane and particle, causing a structural modification through exchange or direct mixing of phospholipids of particle and plasma membrane. For all other nanosystems (including naked macromolecular therapeutics and nanocarrier systems) energy dependent route are used (Panariti, Miserocchi et al. 2012).

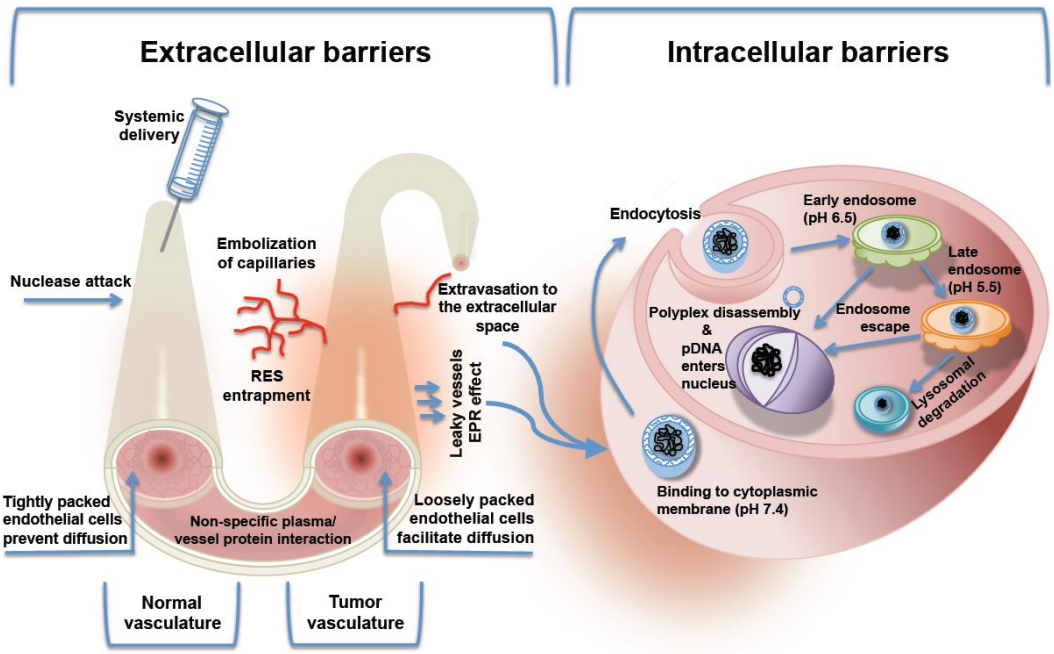

Figure 2.1. Systemic barriers to delivery vehicles
(Source: McCrudden and McCarthy 2013)

Endocytosis is the basic process used for internalizing molecules by cells. Its role is not limited with uptaking of nutrients. One of the important roles of the endocytosis mechanism is regulation of surface receptors. Certain bacteria and viruses also use this pathway in entering the cell (Canton and Battaglia 2012). In the endocytosis process, the internalized material wrap the positioned region of the plasma membrane, plasma membrane extends outward and surrounds the foreign material. Coated vesicle starts to deepen into the cell interior. The first station of endocytic pathway is early endosome, where environment is mildly acidic. Generally cargos arrive in 5 min and return to the plasma membrane. Therefore, it has a rapid recycling character in 5-10 min. Next station is late endosome which has acidic environment. Cargos generally arrive in 60 min. Instead of the late endosome, some substances like apotransferrin can be recycled in recycling endosome to the plasma membrane after 30 min. The last compartment of the endocytic pathway is lysosomes. In lysosomes, the pH is 4.5 and lysosomal enzymes more than 60are involved. In here most substances can be degraded (Duncan and Richardson 2012). Some of the protein drugs could be only delivered to cytosol less than 5 % due to endocytosis (Berg, Selbo et al. 1999). In intracellular transport cytoskeleton has an important role. Intermediate filaments, microtubules and actin filaments are the constituents of the cytoskeleton of the most

eukaryotic cells. Some myosins, the motors of actin and microtubule, urge short-range movements through actin-rich area before transport throughout microtubules in endocytosis (Soldati and Schliwa 2006). The most prominent factor of the formation of phagosomes and macropinosomes is actin polymerization. Moreover, lots of myosin isoforms are used in these formations (Panariti, Miserocchi et al. 2012). The uptake mechanisms are shown in Figure 2.2.

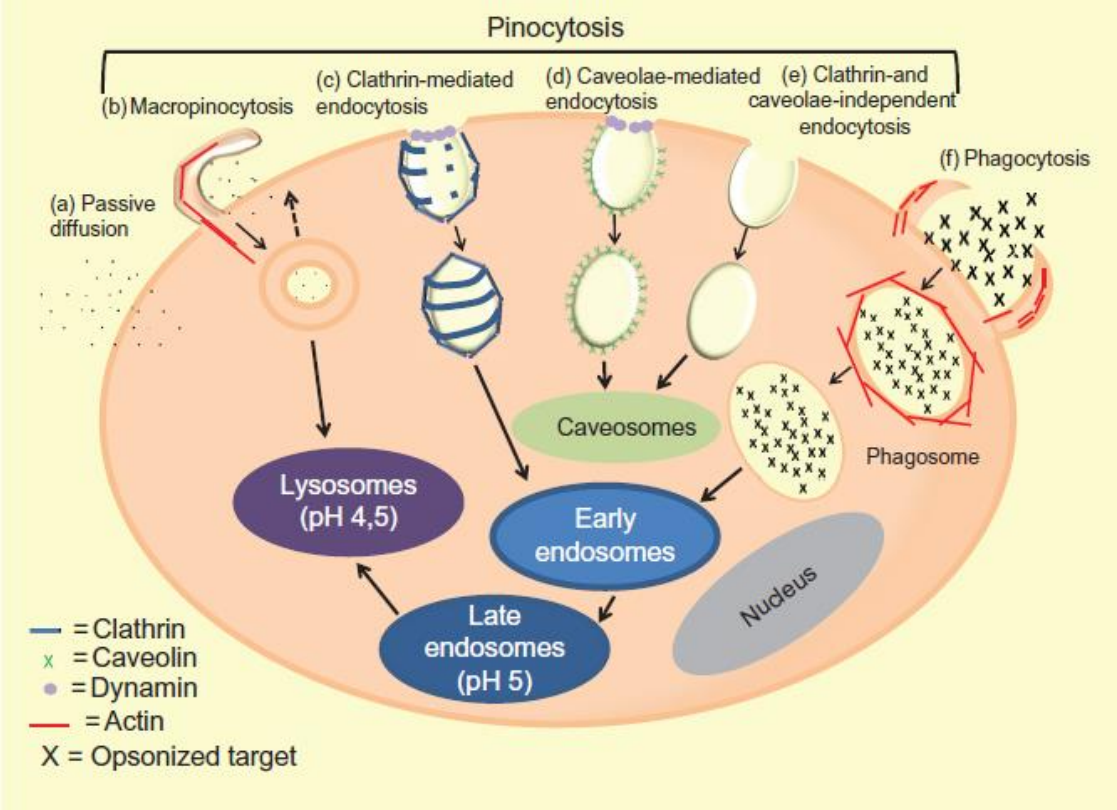

Figure 2.2. Passive and active uptake mechanisms
(Source: Panariti, Miserocchi et al. 2012)

Macromolecular therapeutics need delivery vehicles or vectors, for escaping endo-lysosome pathway and reaching intracellular sites. The two main types of vectors are viral vectors as natural vectors involving bacteria and viruses, and non-viral vectors as synthetic vectors including liposomes, cationic polymers, amphiphilic peptides, polymersomes and lipids (Canton and Battaglia 2012). Despite differences of ways used by enveloped and non-enveloped viruses, generally, viral vectors are uptaken through the cell-membrane via their integral surface proteins. Pore formation/membrane disruption mechanisms are used by non-enveloped viruses (Broeckling, Broz et al.

2008). On the other hand, enveloped viruses use lowering endosomal pH mechanisms (Mudhakir and Harashima 2009). In addition intracellular bacteria use pore-forming toxins activated with the lowering pH and this toxins cause degradation of the organelle (Tweten 2005). Although natural vectors are very effective, their mechanisms and potential immunogenicity are still unkown. Furthermore, they have some practical drawbacks such as bulk production and quality control (Canton and Battaglia 2012).

Researchers have designed synthetic polymers, peptides and lipids which mimic endosomal escape strategies of the viral vectors. (McCrudden and McCarthy 2013). The non-viral systems have pros and cons, as well. The advantage of these systems is safety. Unfortunately, they are not as efficient as their viral counterparts (Canton and Battaglia 2012).

The endosomal escape mechanisms of non-viral systems generally involve fusion with membrane, buffering of endosomes and pore formation in the endosomal membrane. These systems have been explained in detail in the following sections.

2.2. Membrane–Disruptive/Destabilizing Systems for Intracellular Drug Delivery

2.2.1. Membrane-Destabilizing Peptides and Proteins

Various natural and synthetic peptides / proteins have been used as membrane-destabilizing agents. Such peptides/proteins can fuse with endosomal membrane and help the release of therapeutic cargo to the cytosol (Joanne, Nicolas et al. 2009).

The first example of the natural membrane-destabilizing pathogens is HGP. This peptide has 24 amino acids derived from HIVgp41. This peptide efficiently increases the endosomal escape when binding to gene delivery vehicle. However, synthesis of HGP via solid phase has many difficulties. Since the length of this peptide is long and it is hydrophobic, the overall synthesis yield is usually low (Kwon, Liong et al. 2010).

The other example is HA-2 hemagglutinin. The N-terminal fusogenic peptide (a hydrophobic fusion peptide) has a random coil shape. This peptide is derived from influenza virus which uses the conformational change for endosomal escape. The acidic character of the endosome act as a trigger for the protonation of carboxylate groups of amino acid residues on the peptide. The hydrophilic character of the peptide turns to

hydrophobic which fuses with the endosomal membrane (Harrison 1995, Knipe, Samuel et al. 1996), (White 1992),(Wagner, Plank et al. 1992).

Another example is TAT-fusion peptide from HIV-1. TAT protein transduction domain is widely used in intracellular drug delivery systems. The mechanism is not completely known. It was supposed that this peptide directly binds to membrane, which is not dependent on energy and temperature. However, Wadia et al. proved that ionic interactions between cellsurface and the peptide firstly take place. TAT-fusion proteins then penetrate rapidly via lipid raft-dependent macropinocytosis. Transduction is not dependent on interleukin-2 receptor/raft-, clathrin-mediated, caveolar- endocytosis and phagocytosis. In the light of this information, a transducible, fusogenic, pH-sensitive dTAT-HA2 peptide that can escape from macropinosomes was developed (Wadia, Stan et al. 2004).

Contrary to fusion viruses, non-enveloped viruses use receptor mediated endocytosis. They are not internalized via membrane fusion mechanism. Hence, these viruses lyse the endosomal membrane to release into the cytoplasm (Greber, Singh et al. 1994) (Knipe, Samuel et al. 1996). Shenk et al. showed that human adenovirus 2 uses viral fiber to bind cell surface receptor followed by the binding of penton-base protein integrin receptor. After the dissociation of the fibers, viral particles can be uptaken by coated vesicles. Because of acid-activated lytic behavior of the penton-base protein, the virus particles can lyse the endosomal membrane and escape into the cytoplasm (Shenk 1996). These adenoviruses are widely used in synthetic vectors to prevent DNA degradation in the lysosome as well (Michael and Curiel 1994).

L240 peptide from papilloma virus L2 minor capsid protein has been used in neuron targeted-nucleic acid delivery systems. Neuron targeted delivery is important and difficult because neurons use specific and unique pathways. Thus, transfecting of neurons with non-viral vectors is difficult. This peptide was used with a polycation in a multicomponent delivery vehicle (Kwon, Bergen et al. 2008).

Cationic peptides can neutralize, condense and wrap with pDNA which mimics viral fusion proteins. Szoka et al. synthesized a synthetic peptide which is composed of glutamic acid alanine-leucine-alanine sequence repeat. GALA has hydrophobic units, i.e.apolar leucine residues.Glutamic acid which is a polar acidic residue gives GALA a pH-sensitive character and negative charge. At acidic conditions in endosome glutamic acid units are protonated and the peptide adopts a helix conformation which destabilizes endosome membrane. GALA has been often used to deliver DNA to cells. GALA

includes the sequence of glutamic acid–alanine–leucine–alanine. Leucine residues are apolar which brings hydrophobicity to peptide, however glutamic acid is polar giving pH-sensitive character to the peptide. Glutamic acid residues are protonated at lower pH and gains a helix state and leucine parts exist on the protonated glutamic acid sides to generate hydrohobic part in the endosomal compartment. GALA causes membrane fusion (Wyman, Nicol et al. 1997).

Szoka et al. claims that KALA fusogenic peptide is the first "all-in-one" peptide due to the presence of positively charged lysine residues which facilitates binding with nucleic acids. KALA is simply a derivative of GALA as GALA is a negatively charged peptide that cannot directly bind with DNA. In the endosomal compartment, KALA has an α-helix conformation.(Wyman, Nicol et al. 1997) KALA has been used to deliver genes to hepatoma cells (Han and Il Yeom 2000), such as HEK293T and HepG2 cells (Chen, Zhuo et al. 2010).

One of the improvements in this field is the development of multi-domain peptidic biomimetic vectors to deal with barriers such as endosomal entrapment, serum nucleases and nuclear localization. Tumour related apoptosis inducing ligand (TRAIL) was delivered by such biomimetic vectors (Mangipudi, Canine et al. 2009). Inducible nitric oxide synthase (iNOS) pDNA was also delivered toZR75-1 breast cancer cells in vitro (McCarthy, Zholobenko et al. 2011).

Unfortunately, all these peptide-based systems have serious drawbacks. The most important disadvantage is the immunogenic property of the peptides. The bulk production of these systems is also very difficult.

2.2.2. Membrane-Disruptive Polymers

Beside the pros of the membrane-disruptive peptides, the potential problems of these peptides have led to studies toward the development of new, better systems for intracellular drug delivery. Consequently, polymeric nonviral vectors that mimic membrane destabilizing capacity and pH-sensitivity of natural and synthetic peptides have been developed. Membrane destabilizing polymers have advantages such as lower toxicity and immunogenicity, industrial production and higher gene-packaging capacity than peptide systems and natural genetic material (Lollo, Banaszczyk et al. 2000).

2.2.2.1. Membrane-Disruptive Polycations

Membrane-disruptive polycations have been used especially in intracellular delivery of genes since they usually have positively charged amine groups which can form electrostatic complexes with nucleic acids. Most of polycations such as poly(ethylene imine) (PEI), poly(2-(dimethylamino)ethyl methacrylate) (PDMAEMA), a polysaccharide chitosan, spermine-modified dextran have been used as vehicles for delivery of pulmonary genes (Figure 2.3).

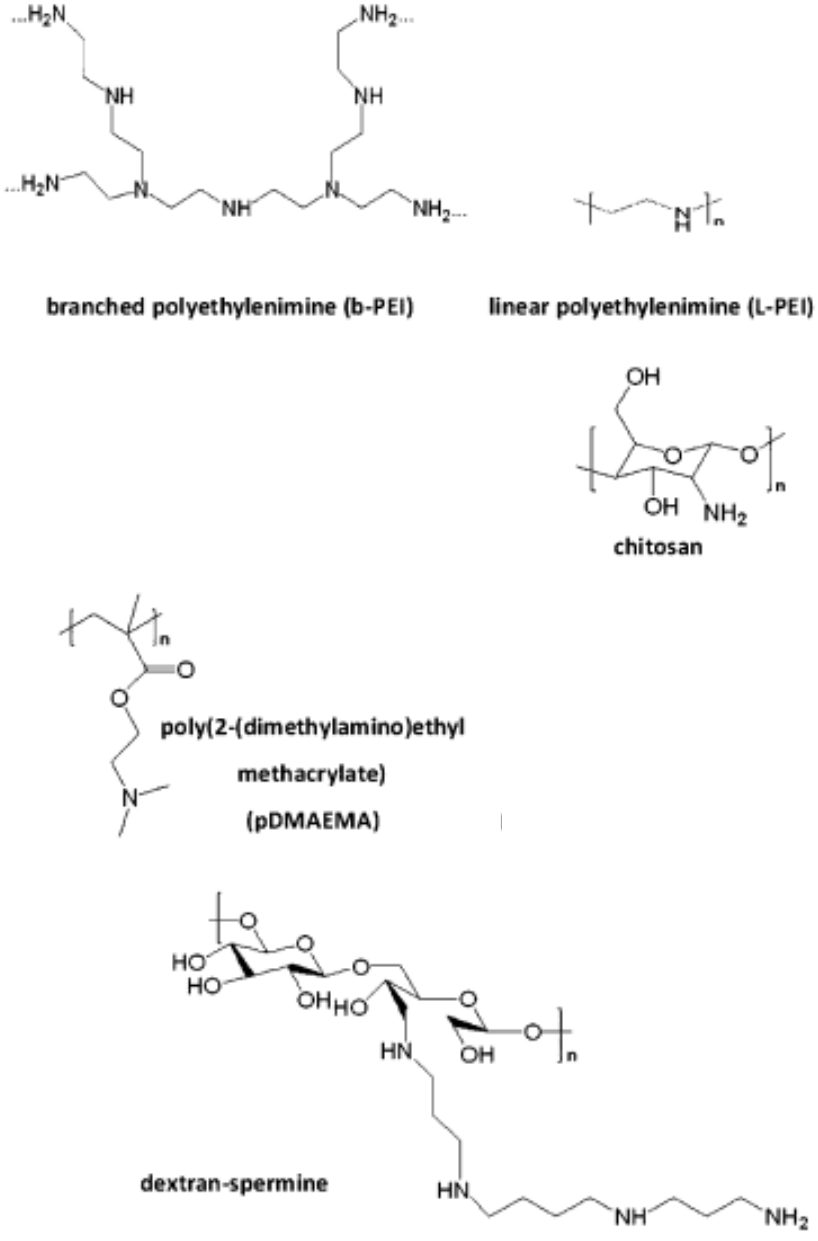

Figure 2.3. Membrane-disruptive polycations
(Source: Merkel, Zheng et al. 2011)

Poly(ethylene imine) (PEI) was first discussed as a gene delivery vehicle in 1995 (Boussif, Lezoualc'h et al. 1995). Scientists were able to synthesize PEI with varying molecular weights ranging from 1kDa to 1.6x10^3 kDa (Baker, Saltik et al. 1997), (Meunier-Durmort, Grimal et al. 1997). In transfection studies with L929 cells, it was found that the most suitable molecular weight of this polymer as a gene delivery vehicle is between 5 and 25 kDa. Cytotoxicity of PEI increases with increasing molecular weight, because higher molecular weight PEI aggregates with cell surface. Low molecular weight PEI has less toxicity however less effective in gene delivery due to lower number of positive charges causing difficulty in condensing the negatively charged DNA (Godbey, Wu et al. 1999). The proton-sponge capacity of PEI is vital for the endo-lysosomal escape. Proton sponge effect is a buffering effect. The protonable amine groups are protonated in endosomal compartment which causes flux of protons and chloride ions into the compartment. Osmotic pressure difference and swelling of compartment occurs which ruptures endosome.

A natural amine, spermine exists in all eukaryotes necessary for cell growth and its amino groups are positively charged at physiological pH. It has high transfection efficiency, biocompatibility and nucleic acid condensing capacity (Du, Chen et al. 2012). Dextran-spermine polymer synthesized to control the conditions of gene expression of D-SPM/plasmid DNA. (Abdullah, Wendy-Yeo et al. 2010) Dextran-spermine conjugates show transfection efficiency dependently ratio of grafted spermine. The primary and secondary amines of spermine supply a proton-sponge capability in acidic medium of endosome and endosomal splitting.

Lastly, a new spermine-like polymer was synthesized by Kurtulus et al. In this study, a new methacrylate monomer that 2-((tert-butoxycarbonyl) (2-((tert-butoxycarbonyl) amino) ethyl) amino) ethyl methacrylate (Boc-AEAEMA) was polymerized via reversible addition-fragmentation chain transfer (RAFT) polymerization. The *in vitro* cytotoxicity and proton sponge effect of deprotected polymers P(AEAEMA)’s were investigated and compared with those of PEI. It was found that P(AEAEMA) is as effective as PEI in proton sponge effect and also PEI is much more toxic than P(AEAEMA) (Kurtulus, Yilmaz et al. 2014).

2.2.2.2. Membrane-Disruptive Polyanions

Polyanions are used widely as alternatives to viral vectors. Polyanions have acidic groups as functional groups. Some examples of polyanions include polyacrylic acid (PAA) and polymethacrylic acid (PMAA). Membrane-disruptive polyanions generally involve carboxylic or sulfonic acid groups and also hydrophobic groups that facilitate membrane-destabilization at acidic conditions. Polyacids are pH-sensitive, i.e. they give response to small changes in the pH of the environment. These responses are reversible. At lower pHs the acidic group of the polyanions are protonated while they release their protons at higher pHs. (Almeida, Amaral et al. 2012). As pH is higher than the pKa of the functional acidic groups, ionic repulsion occurs which results in the formation of an extended coil conformation. At a pH lower than the pKa attraction forces exist between lipid membranes and polymer chains through the hydrophobic interactions (Tonge and Tighe 2001). As an example to membrane-disruptive polyanions, alkylamide derivatives of poly(styrene-alt-maleic anhydride) (PSMA) can be shown. As seen in Figure 2.4, Hoffman and co-workers synthesized propylamine, butylamine and pentylamine derivatives of PSMA at different molecular weights (40 kDa, 60kDa and 80 kDa). The propylamine derivatives show no hemolytic activity. Increase in alkyl chain length increases hemolytic activity at pH 5.8 while no hemolysis at neutral pH occurs since at neutral pH hydrophobicity decreases due to the deprotonation of acidic units, thus interaction with red blood cells decreases. Hence, the most hemolytic activity belongs to pentylamine derivatives at both pH 6.6 and pH 5.8. At 5.8 the hemolytic activity is higher than that at pH 6.6. Importantly, increase in molecular weight increases hemolytic activity (Henry, El-Sayed et al. 2006).

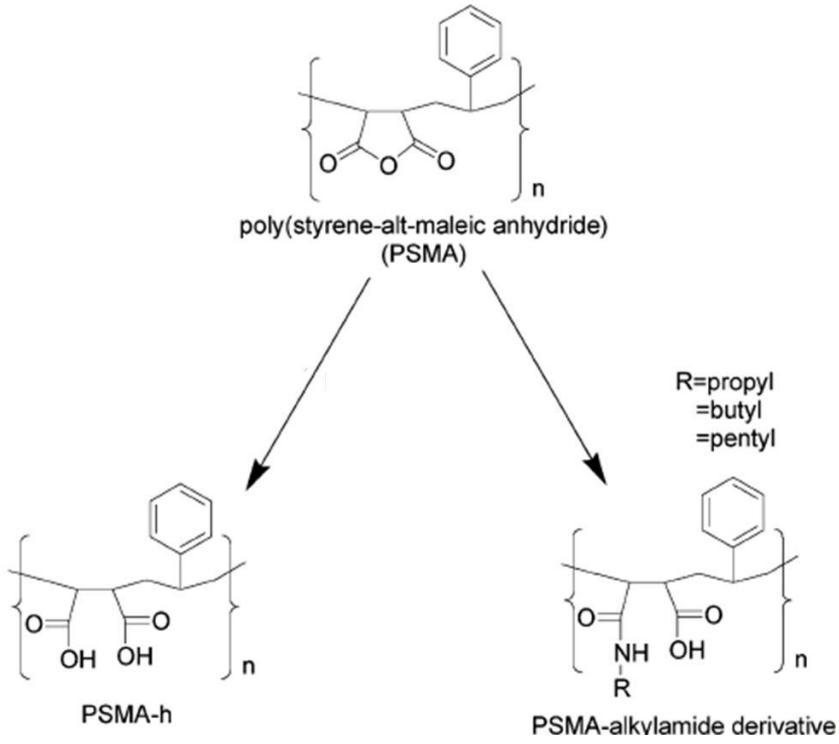

Figure 2.4. PSMA and PSMA-alkylamide derivatives
(Source: Henry, El-Sayed et al. 2006)

It was shown that lipid vesicles were disrupted by poly(ethylacrylic acid) (PEAA) in a pH-dependent manner PEAA strongly interacts with lipid membranes at acidic environment. Hoffman and co-workers designed a series of polymer compositions to show pH-dependent membrane disruptive activity of increasing hydrophobicity with increasing the length of alkyl group. PEAAc was found to have an hemolytic activity of 10^7 molecules per red blood cell as effective as peptide melittin. At neutral pH, PEAAc shows no hemolytic activity. When decreasing pH from 6.3 to 5.0 which mimics the transition fromearly to late endosomal compartments, hemolytic activity of PEAAc increases sharply. Moreover, a more hydrophobic polymer with one additional methylene group, i.e. poly(propyl acrylc acid) (PPAAc) shows hemolytic activity 15 times more than PEAAc at pH 6.1 and no hemolysis at neutral pH. 1:1 random copolymers of ethyl acrylate (EA) and acrylic acid (AAc) have similar structure with PEAAc has closely effective hemolytic activity with PEAAc (Murthy, Robichaud et al. 1999).

Bulmus et al synthesized pyridyl disulfide acrylate and random copolymers of this monomer with methacrylic acid and butyl acrylate (poly(MAA-co-BA-co-PDSA)) which showed pH-sensitive membrane disruptive activity. Besides the membrane

disruptive behavior, intracellular distribution and cytotoxicity of these terpolymers were tested. Poly(MAA-co-BA-co-PDSA) was found to be hemolytic active at low pHs and nontoxic on 3T3 fibroblast and THP-1 macrophage like cells. The uptake and enhanced cytoplasmic delivery of the polymer was also demonstrated (Bulmus, Woodward et al. 2003).

Sevimli et al. synthesized well-defined poly(methacrylic acid-co-cholesteryl methacrylate) P(MAA-co-CMA) as a nonviral pH -sensitiveagent for intracellular drug delivery. Cholesterol was used as a hydrophobic component on the polymer backbone to facilitate interaction with lipid membranes. Characterization of different statistical copolymers with varying cholesterol content (2%,4% and 8 % mol) shows that 2 and 4 % mol CMA content copolymers in aqueous solution are present as unimers, however 8 % mol CMA content copolymer organizes into supramolecular structures in aqueous solution. The interactions with lipid membranes were shown in a pH-dependent manner (at pH5.0 and 7.4) via SPR and liposome leakage assay. 2 mol % CMA containing copolymer showed the most lipid membrane interaction at pH 5.0 and membrane disruptive activity (Sevimli, Inci et al. 2012).

2.3. Lipid Based Membrane-Disruptive Systems

Lipid based systems have an important role in intracellular drug delivery. There are many examples of cationic lipids which were the first subtances that were used to make complexes with pDNA for nonviral gene delivery. Felgner revealed that N-[1-(2,3-dioleyloxy)propyl]-N,N,N- trimethylammonium chloride (DOTMA) could be complexed with DNA because of the interactions between the positively charged amine groups on the lipid and the negatively charged phosphate groups on DNA. (Felgner, Gadek et al. 1987) Various cationic lipids have been used in gene delivery. Most of them can encapsulate pDNA. Dioctadecylamidoglycylamidoglycylspermine (DOGS), [1,2-bis(oleoyloxy)-3-(trimehylammonio)propane] (DOTAP) AND 3β[N-(N',N'-dimethylaminoethane)-carbamoyl] cholesterol (DC-Chol) are a few examples of cationic lipids (Behr, Demeneix et al. 1989), (Leventis and Silvius 1990), (Gao and Huang 1991). Addition of cholesterol and dioleoylphosphatidylethanolamine (DOPE) as helper lipids or co-lipids increases transfection efficiency (Kurosaki, Kitahara et al. 2009). Caracciolo et al. synthesized DOTAP-DOPC/DNA and DOT AP-Chol-DOPC-

DOPE/DNA lipoplexes for transfection. The effect of the combination of cationic lipids and helper-lipids mechanisms is not known well (Caracciolo, Caminiti et al. 2009).

1- palmitoyl – 2 – oleoyl – sn – glycerol - 3- ethyl phosphocholine (EPOPC) : cholesterol liposome with folate electrostatically-associated was used for delivery of HSV-tk suicide gene. Tumor growth delay was observed with this system (Duarte, Faneca et al. 2012).

The drawback of lipid-based systems and lipoplexes is instability in serum similar to poly(propylacrylic acid) (PPAA) and toxicity (Sternberg, Hong et al. 1998), (Filion and Phillips 1997), (Kiang, Bright et al. 2004).

2.3.1. Cholesterol Containing Systems

Cholesterol is widely used in drug delivery due to its ability to cross cellular membranes (Sevimli et al.). Wolfrum et al. synthesized liphophilic siRNA conjugates in order to determine the efficient *in vivo* delivery of siRNA. Cholesterol, stearoyl, myristoyl, lauryl, oleoyl, lithocholeic-oleoyl, palmitoyl and docosanyl were used in siRNA–liphophilic conjugates shown in Figure 2.5. All of these lipids had different hydrophobic chain length. Cholesterol conjugated siRNA suppressed apoB mRNA levels and decreased plasma apoB levels and serum cholesterol. The most effective conjugate was found to be cholesterol based.

Docosanyl showed similar effect with cholesterol. Stearoyl and lithocholeic-oleoyl had lower activity than both cholesterol and docosanyl conjugates. In addition, cholesterol is transported with lipoprotein particles including amphiphilic phospholipids which providing the solubility in the circulation. These lipoproteins are high-density lipoprotein (HDL) and low-density lipoprotein (LDL). HDL caries reverse cholesterol from peripheral tissues to tissues other lipoproteins in which both endocytosis-dependent and endocytosis-independent lipid uptake mechanisms are used. The most popular HDL receptor is scavenger receptor class B, type I (SR-BI). However, LDL carries cholesterol extracellularly to the other tissues. Hepatocytes take LDL cholesterols via LDL receptor-mediated endocytosis with interaction of apoliprotein B100 (apoB-100). After endocytosis, free cholesterol is released by lysosomal enzyme and recycled the LDL receptor to the cell surface. In this study, it was shown that the cholesterol-siRNA which carried by HDL is 8 to 15 times more efficient at silencing

apoB protein expression in vivo comparing with cholesterol-siRNA (Wolfrum, Shi et al. 2007).

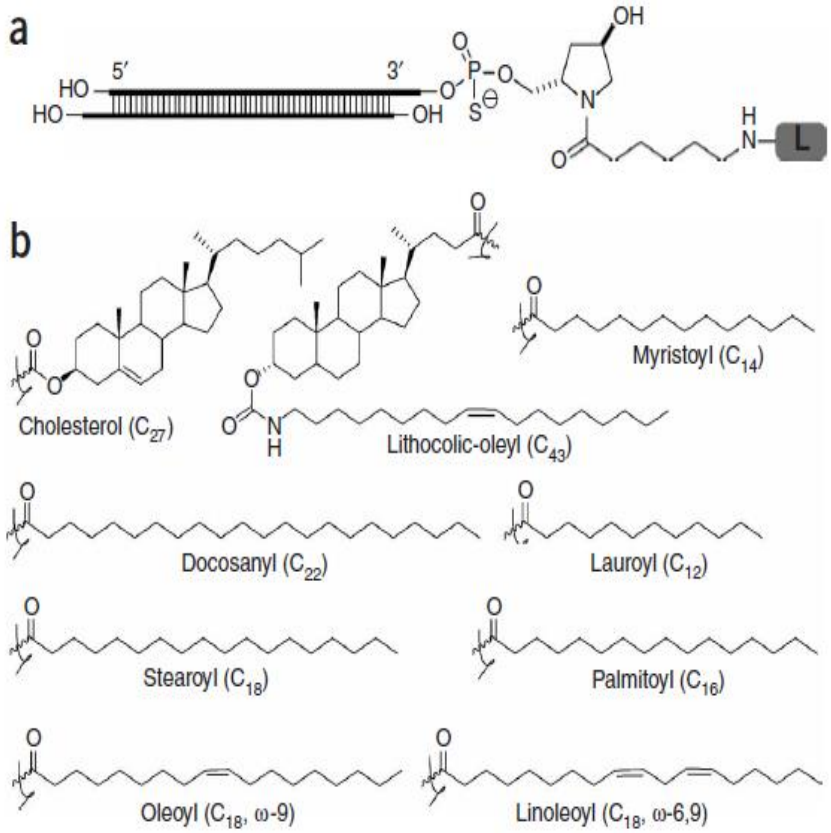

Figure 2.5. Lipophilic siRNAs
(Source: Wolfrum, Shi et al. 2007)

In another study, cholesterol (cho) and poly(N,N-dimethylaminoethylmethacrylate) (PDMAEMA) were used with lecithin liposomes. According to flow cytometry results, lecithin-cho lipoploexes had higher uptake than lecithin by Caco-2 and TC7 cells. In addition, these complexes were pH-responsive. At neutral pH, there was no calcein release from lipoplexes. At acidic environment 100 % calcein release was found. The uptake mechanism is not known (Alves, Hugo et al. 2013).

Sevimli et al. synthesized statistical poly(dimethylamino ethyl methacrylate-co-cholesteryl methacrylate) P(DMAEMA-co-CMA) via reversible addition-fragmentation chain transfer (RAFT) polymerization. Uv-Vis spectroscopy and DLS results revealed pH-responsive behavior of these copolymers. According to potentiometric studies, besides the cationic charge, cholesterol content affected buffering capacity and pKa values of copolymers. Lower cholesterol content copolymers showed higher

cytotoxicity. P(DMAEMA-co-CMA) polymers were found to be potential siRNA delivery agents (Sevimli, Sagnella et al. 2012).

Yinsong et al. synthesized pH-sensitive pullulan based nanoparticles with conjugation of uronic acid as a pH-sensitive moiety and cholesterol succinate as a hydrophobic moiety. UCPA-1 nanoparticles with the ratio of substitution with urocanyl and cholesterol of 6.8 and 3.5, respectively, had high drug loading capacity and in vitro pH-induced drug release activity. This nanoparticulate system increased the cytotoxic effect of DOX in MCF-7 cells (Wang, Liu et al. 2014).

CHAPTER 3

MATERIALS AND METHODS

3.1. Materials

Cholesterol and methacryloyl chloride were purchased from Aldrich. t-BMA was purchased from Sigma and used after purification wih basic alumina column chromatography. N-Hydroxyethylethylenediamine (99%) and di-*tert*-butyl dicarbonate were purchased from Aldrich to use in the synthesis of *tert*-butyl (2-((tert-butoxycarbonyl)amino)ethyl)(2-hydroxyethyl)carbamate according to the procedure reported by Kurtulus et al. 2,2'-Azobis (2-methylpropionitrile) (AIBN) (Fluka) was used after recrystallization twice in methanol. Chain transfer agent, 4-cyano-4-(phenylcarbonothioylthio) pentanoic acid (CPADB) was purchased from Aldrich. Silica gel (pore size 60 Å, 70- 230 mesh) was purchased from Fluka. Acetic acid, sodium acetate, citric acid and mono and dibasic phosphate salts were used to prepare buffer solutions and purchased from Merck. Hydrochloric acid and sodium hydroxide were purchased from Merck and Sigma, respectively.

Polyethyleneimine (Mn: 25 and 60 kDa) was purchased from Aldrich and Fluka, respectively. Toluene, ethyl acetate, hexane, dichloromethane (DCM), trifluoroacetic acid deuterium oxide (D2O), deuterium chloroform (CDCl3), triethylamine (TEA), hexylamine, diethylether, methanol and N'N-dimethylacetamide (DMAc, HPCL grade ≥ %99.9) were purchased from Sigma. Dialysis membrane (MWCO= 500-1000 Da) was purchased from Spectrum® Laboratories. DMEM (Dulbecco's Modified Eagle's Medium) medium, L glutamine, tyripsin and Foetal Bovine Serum (FBS) were obtained from Gibco. Phosphate buffer saline, (PBS) solution pH 7.1, 0.1 mM) was prepared using relevant mono and dibasic salts and NaCl. Thiazolyl Blue Tetrazolium Blue (MTT) reagent was purchased from Sigma-Aldrich. Epithelial (NIH 3T3) cell line was kindly provided by Bioengineering Research and Application Center, İzmir Institute of Technology, İzmir, Turkey. Oregon Green® 488 maleimide and 4',6-diamidino-2-phenylindole (DAPI) dilactate dyes were purchased from Invitrogen Molecular Probes.

3.2. Instruments

3.2.1. Nuclear Magnetic Resonance Spectroscopy

Nuclear Magnetic Resonance Spectrometer (Varian, VNMRJ 400 MHz) was used to determine the chemical structure of synthesized compounds and the conversion of the monomers to polymers using deuterium oxide (D_2O) and deuterated chloroform ($CDCl_3$) as NMR solvents. For analysis, samples were dissolved at 6 to 10mg/ml concentration in both D_2O or $CDCl_3$ depending on the solubility of the samples.

3.2.2. Gel Permeation Chromatography

The molecular weight and molecular weight distribution of cholesteryl methacrylate-co-t-butyl methacrylate copolymers were determined by gel permeation chromatography (GPC) at Bogazici University (İstanbul, Turkey) using THF as mobile phase. The THF GPC Viscotek GPCmax VE-2001 analysis system was equipped with PLgel (length/ID 300 mm × 7.5 mm, 5 μm particle size) Mixed-C column calibrated with polystyrene standards, and a refractive index detector . Cholesteryl methacrylate-co-2-((Tert-butoxycarbony)(2-((tert-butoxy carbonyl)amino)ethyl)amino)ethyl Methacrylate (P(CMA-co-Boc(AEAEMA) copolymers were analyzed by GPC using N,Ndimethylacetamide (DMAc) containing 0,05 % w/v LiBr as a mobile phase. DMAc GPC was a Shimadzu, brand modular system comprising an SIL-10AD auto injector, PSS Gram 30 Å and 100 Å (10 μM, 8x100 mm) columns, a RID-10A refractive-index detector and SPD-20A prominence UV/Vis detector calibrated with low polydispersity poly(methyl methacrylate) standards (410-67000 g/mol).

3.2.3. UV-Visible Spectroscophotometry and Dynamic Light Scattering Particle Analyzer

UV-visible light absorbance of the solutions was measured using a Thermo Scientific Evolution 201 UV-visible spectrophotometer in the range between 200 nm and 600 nm using quartz cuvettes.

Malvern NanoZS Particle Analyzer was used to determine hydrodynamic diameter of polymers, at varying pH values.

3.2.4. Microplate Reader

In hemolysis and cytotoxicity assays, a Thermo Electron Corporation Varioskan microplate reader was used to measure visible light of solutions in 96-well plates.

3.2.5. Fluorescence Microscopy

Olympus BX71 fluorescence microscope was used for intracellular distribution analyses of fluorescent labelled polymers.

3.3. Methods

3.3.1. Synthesis of Cholesteryl Methacrylate (CMA)

Cholesteryl methacrylate (CMA) was synthesized according to procedure reported by Sevimli et al (Sevimli, Inci et al. 2012). Briefly, Cholesterol (2.0g, 0.02 mol) was dissolved in 5 ml of the mixture of triethylamine (3.75 ml) and toluene (12.5 ml). The solution was then refluxed at 60^0 C. Methacryloyl Chloride (3.3 ml, 0.6 ml) was dissolved in the remaining mixture of triethylamine and toluene. The mixture was then added dropwise to the cholesterol solution. The final reaction medium was further refluxed for 12 hours. The solution was let to cool down to room temperature. The product, cholesteryl methacrylate was purified by precipitation in hydrocholoric acid solution (300 ml, 1.6 N) in methanol. Finally, obtained white precipitate was dried in vacuo overnight.

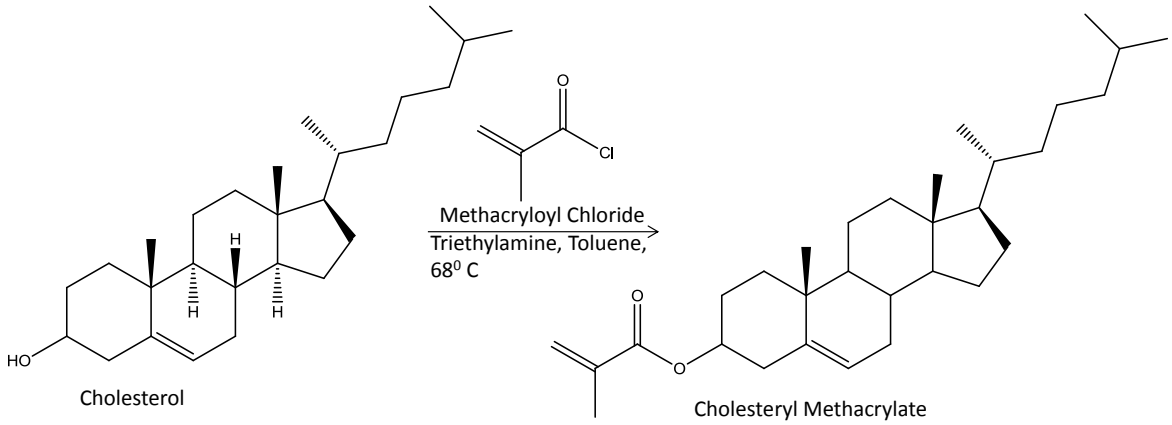

Figure 3.1. Synthesis of CMA monomer

^{1}H NMR ($CDCl_3$, 400 MHz), ppm: 6.1, 5.5 (m, 2H, C**H$_2$**=C(CH_3)COO-), 5.3 (d, 1H, -C=C**H**-, olefin group in cholesterol), 4.6 (m, 1H, -COO-C**H**-), 1.9 (s, 3H, -CH_2=C(C**H$_3$**)COO-), 0.93 (d, 3H, -CH-C**H$_3$**), 0.88, 0.84 (d, 3H, -CH-(C**H$_3$**)$_2$), 0.68 (s, 3H, -C-C**H$_3$**).

3.3.2. Synthesis of 2-((Tert-butoxycarbony)(2-((tert butoxycarbonyl) amino) ethyl) amino) ethyl Methacrylate (Boc-AEAEMA)

This monomer was synthesized according to the procedure reported by (Kurtulus, Yilmaz et al 2014). The synthesis is shown in Figure 3.2. Firstly, the primary and secondary amine groups of N-(2-hydroxyethyl) ethylenediamine was first protected using di-*tert*-butyl dicarbonate to prevent the reaction of amine groups instead of the alcohol group. N-(2-Hydroxyethyl)ethylenediamine (0.024 mol, 2.43 ml, Mw: 104.15 g/mol) was dissolved in dry DCM (40 ml) at -10°C. After dissolving di-*tert*-butyl dicarbonate (0.048 mol, Mw: 218.25 g/mol) in dry DCM (40 ml). This solution was added dropwise into N-(2-hydroxyethyl)ethylenediamine solution at -10°C. The final solution was purged with nitrogen for about 3 hours and stirred for 24 h at room temperature. Tert-butyl hydrogen carbonate formed as a minor product which was separated by filtration in DCM. Water-DCM extraction was performed 3 times to remove the unreacted N-hydroxyethylethylenediamine. The organic phases were collected and the solvent was removed using a rotary evaporator.

Tert-butyl-2-((tert-butoxycarbonyl) amino) ethyl) (2-hydroxyethyl) carbamate (**1**, BocAEAE) (0.0161 mol, Mw: 304.38 g/mol) was dissolved in dry DCM (40 ml) at 0°C. Triethylamine (TEA, 0.0432 mol) was added dropwise into the solution under N_2 with stirring for 30 min. Finally, methacryloyl chloride (MACl, 0.0288 mol) was added into the solution. The final solution was stirred at 0°C for 4 h under N_2 and for 15 h at room temperature. The solution was filtered to remove the HCl salt. The reaction solution was washed with brine (three times) and extracted with water three times in order to separate dissolved salt, unreacted methacryloyl chloride and triethylamine. After collecting the organic phases, the solvent was evaporated via rotary evaporator. The final product was dried in vacuum oven. The product was then purified by column choromatography method using hexane and ethylacetate solutions (Hxn:EA=1:0; 10:1; 8:1; 6:1; 4:1; 2:1; 0:1). High purity monomer was collected using a hexane and ethyl acetate mixture at a v/v rato of 4:1. The product, 2-((tert-butoxycarbonyl) (2-((tert-butoxycarbonyl) amino)ethyl) amino)ethyl methacrylate (Boc-AEAEMA; **2**, Figure 3.2), was characterized by ^{1}H NMR spectroscopy using deuterated chloroform (CDCl3) as a solvent.

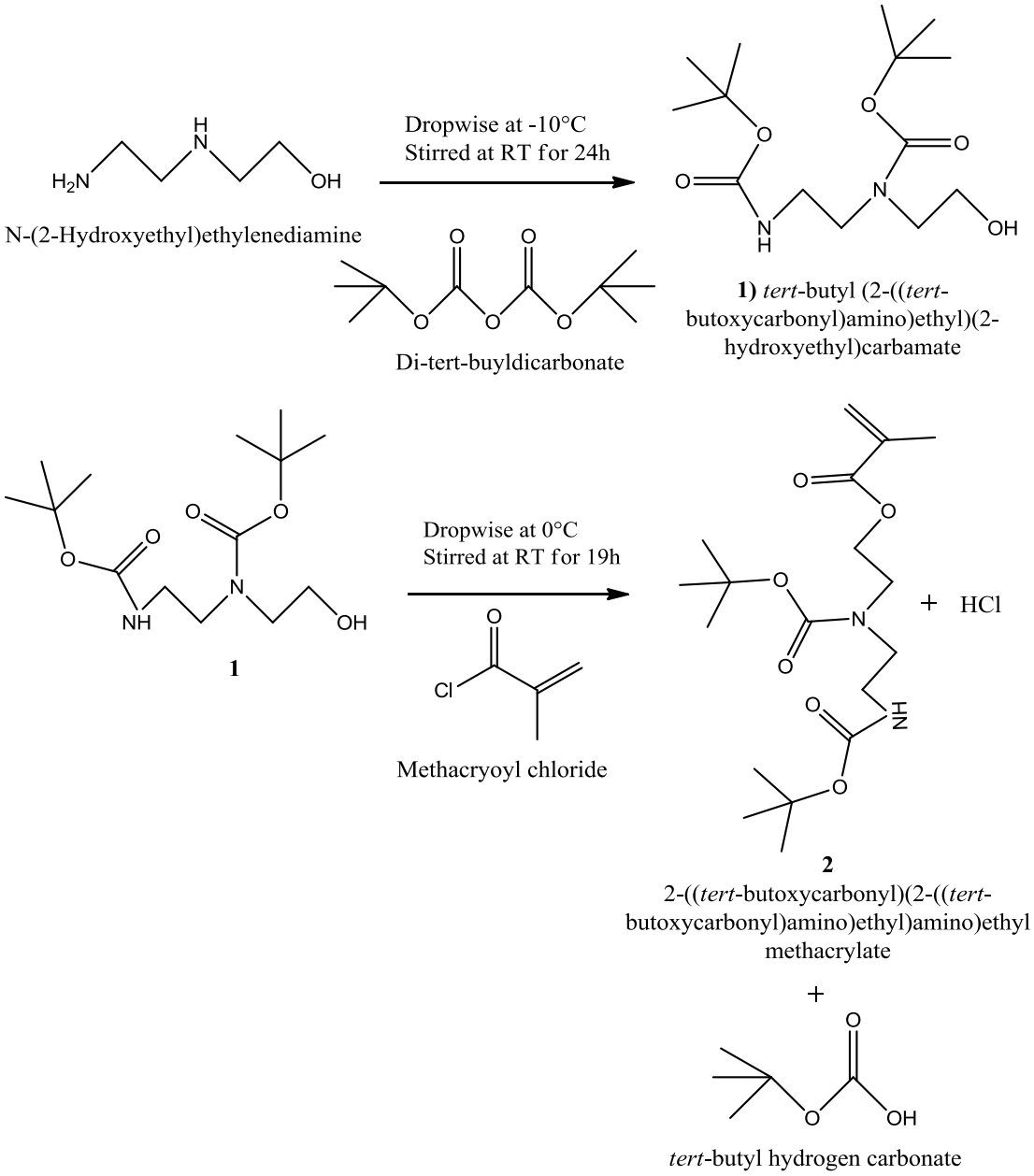

Figure 3.2. Synthesis of 2-((tert-butoxycarbonyl) (2-((tert-Butoxycarbonyl) amino) ethyl) amino) ethyl methacrylate (Boc-AEAEMA)

^{1}H NMR ($CDCl_3$, δ in ppm): 6.11-5.58 (s, 2H, **CH_2**=C(CH3)COO-), 1.94 (s, 3H, C_2=C-**CH_3**), 4.25-4.23 (t, 2H, -COO-**CH_2**-), 3.50-3.27 (t, 6H, -**CH_2**-N(COO(CH_3)$_3$-**CH_2**-**CH_2**-NH(COO(CH_3)), 1.45-1.42 (s, 18H -N(COO-**$(CH_3)_3$**)-CH_2-CH_2-NH-(COO**$(CH_3)_3$**), 4.99-4.79 (s, 1H, -CH_2-**NH**-(COO(CH_3)$_3$).

3.3.3. RAFT Copolymerization of Cholesteryl Methacrylate and t-Butyl Methacrylate

Cholesteryl methacrylate, tert-butyl methacrylate, 4- cyano-4-(phenylcarbonothioylthio) pentanoic acid (CPADB) as raft agent and 2,2'-azobisisobutylnitrile (AIBN) as radical initiator were dissolved in toluene. The copolymerization scheme and conditions are given in Figure 3.3. and Table 3.1, respectively. The solution was degassed with nitrogen for about 30 min in an ice bath. The solution vial was then immersed into a preheated oil bath at 68 ^{0}C. At the end of the polymerization time, after stopping the polymerization by cooling the solution and exposing to air, the solvent was removed in vacuum. Before purification of polymer, conversion of monomer to polymer was analyzed by ^{1}H-NMR spectroscopy in $CDCl_3$.

The copolymers were purified by dissolving in dichloromethane and precipitating in methanol twice. The number average molecular weight and molecular weight distribution were determined with GPC using tetrahydrofuran (THF) as a mobile phase.

^{1}H NMR ($CDCl_3$, 300 MHz) ppm: 5.3 (d, 1H, -C=C**H**-, olefin group in cholesterol), 4.5 (m, 1H, -COO-C**H**-), 2.3 (d, 2H, -CH-C**H**$_2$-), 1.81 (s, 2H, -C-C**H**$_2$-), 1.41 (s, 9H, -C-(C**H**$_3$)$_3$), 1.02 (s, 3H, -C-C**H**$_3$), 0.93 (d, 3H, -CH-C**H**$_3$), 0.88−0.84 (q, 6H, -CH-(C**H**$_3$)$_2$), 0.68 (s, 3H, -C-C**H**$_3$).

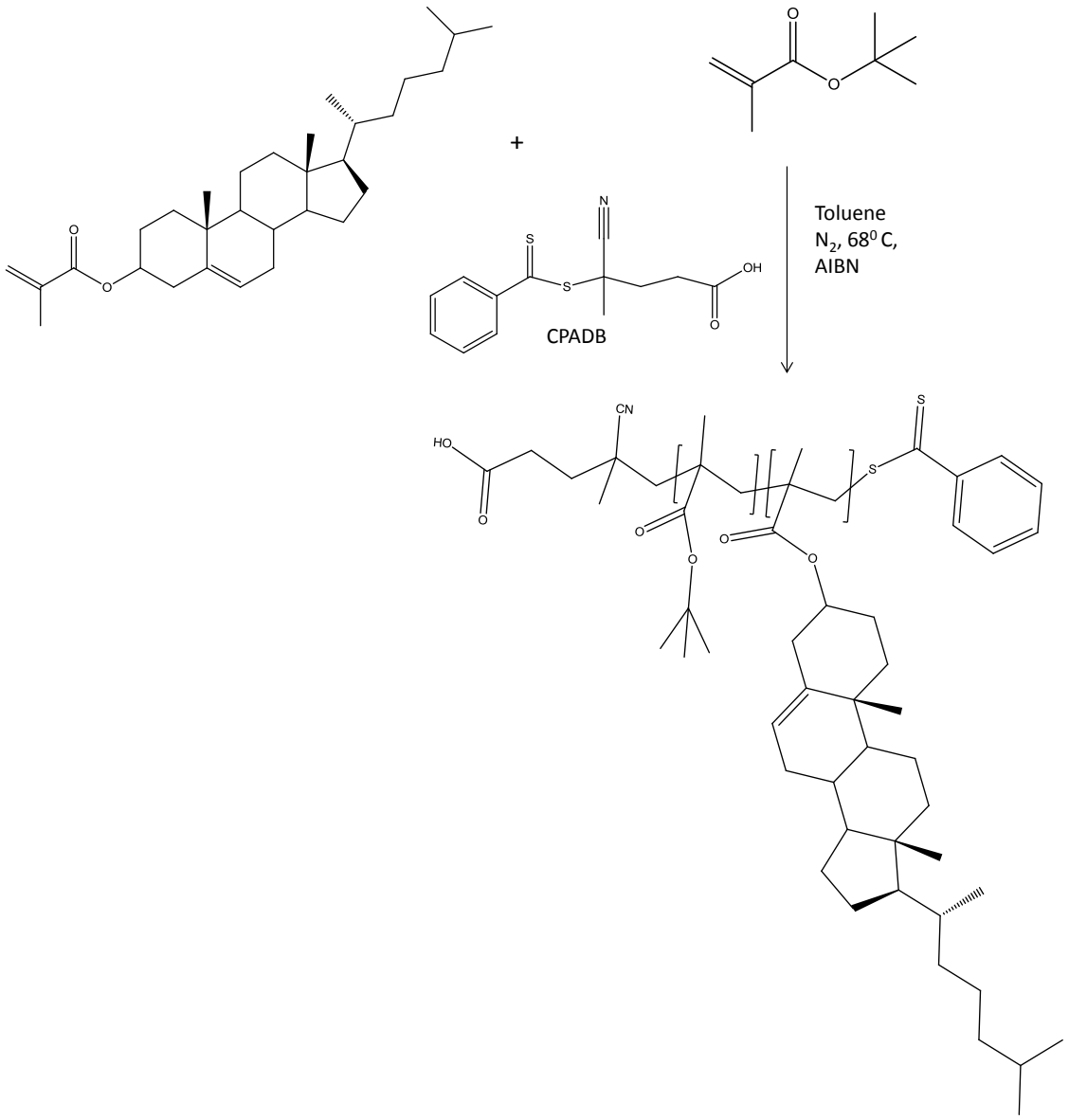

Figure 3.3. Synthesis of copolymers of CMA and t-BMA (p(CMA-co-t-BMA))

The CMA content of copolymers was determined from the H-NMR analysis using Eq 3.1

Table 3.1. Conditions of CMA and t-BMA copolymerizations. Cholesteryl Methacrylate Monomer (CMA), t-Butyl Methacrylate monomer (t-BMA), initiator (AIBN) and RAFT agent (4-Cyano-4-(phenylcarbonothioylthio) pentanoic acid).

Total Monomer Concentration (M)	[t-BMA]/[CMA]/[RAFT]/[AIBN] Mole Ratio	Polymerization time (h)
4.2	490/10/1/0.2	2,4,6,8,18
5.9	490/10/1/0.2	2,3,7,8,12,13,18,19
4.2	490/10/1/0.2	2,4,6,8,18
4.2	480/20/1/0.2	2,4,6,8,18
4.2	460/40/1/0.2	2,4,6,8,18
4.2	450/50/1/0.2	2,4,6,8,18

CMA mol%= [∫a/(((∫v-(48x∫a))/14)+∫a)]x100; t-BMA mol%=[(((∫v-(48x∫a))/14)/(((∫v-(48x∫a))/14)+∫a)]x100.
(3.1.)

P(CMA-co-t-BMA) copolymers were hydrolyzed to p(CMA-co-MAA) copolymers. Copolymer (0.46 M) was dissolved in dichloromethane. Under the vigorous stirring, trifluoroacedicacid (23 M) was added. The solution was reacted for 32 hour at room temperature. After reaction, excess solvent was purged with N_2 gase. The final product was dissolved in 10 mM NaOH solution and transferred into a dialysis tubing (MWCO: 3500 or 1000). The final product p(CMA-co-MAA) was dialyzed against ultra-pure water for 3 days. The final product was obtained after freeze drying as a white powder.

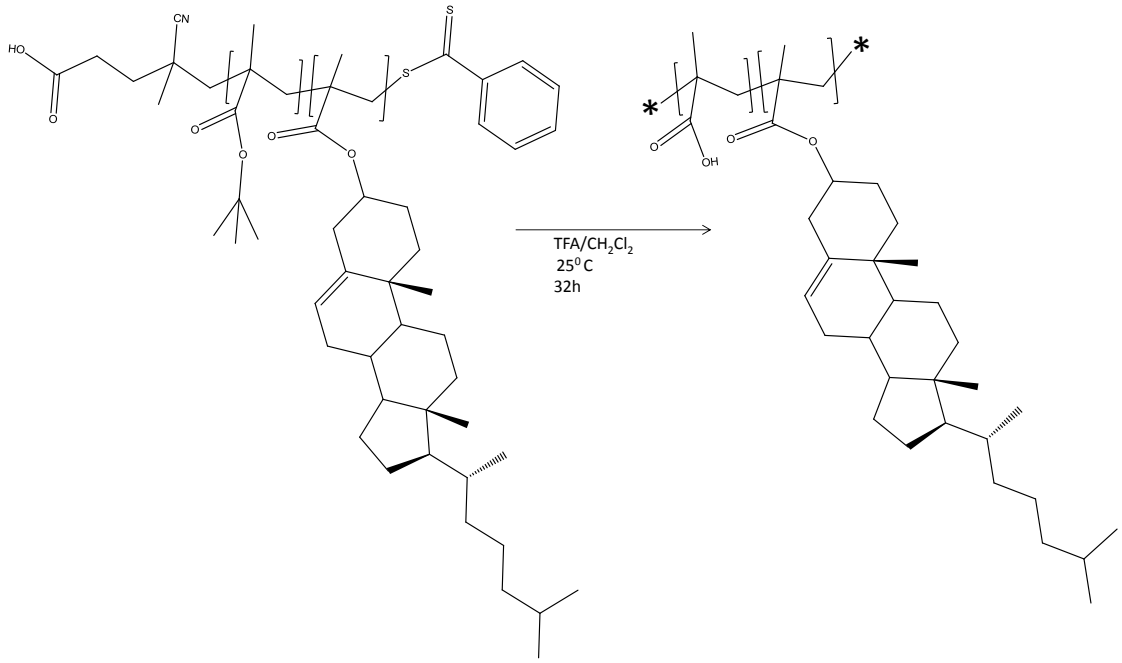

Figure 3.4. Hydrolysis of p(CMA-co-t-BMA) to p(CMA-co-MAA)

^{1}H NMR (DMSO, 300 MHz) ppm: 12.3 (s, 1H, -CO-O**H**), 5.3 (d, 1H, -C=C**H**-, olefin group in cholesterol), 4.5(m, 1H, -COO-C**H**-), 2.3 (d, 2H, -CH-C**H**$_2$-), 1.82 (s, 2H, -C-C**H**$_2$-), 1.02 (s, 3H, -C-C**H**$_3$), 0.93 (d, 3H, -CH-C**H**$_3$), 0.88−0.84 (q, 6H, -CH-(C**H**$_3$)$_2$), 0.68 (s, 3H, -C-C**H**$_3$).

3.3.4. RAFT Copolymerization of Cholesteryl Methacrylate and 2-((Tert-butoxycarbony)(2-((tert-butoxycarbonyl)amino)ethyl)amino)ethyl Methacrylate

Cholesteryl methacrylate, 2-((tert-butoxycarbony) (2-((tert-butoxy carbonyl) amino) ethyl) amino) ethyl methacrylate, 4- cyano-4-(phenylcarbonothioylthio) pentanoic acid (CPADB) as raft agent and 2,2'-azobisisobutylnitrile (AIBN) as initiator were dissolved in toluene. The copolymerization scheme and conditions are given in Figure 3.5 and Table 3.2., respectively. The solution was degassed with nitrogen for about 30 min in an ice bath. The solution vial was then immersed into preheated oil bath at 68 ^{0}C. After polymerization time, the polymerization was stopped by cooling the solution and exposing to air. The solvent was removed in vacuum. Before purification

of polymer, conversion of monomer to polymer was analyzed by ^{1}H-NMR spectroscopy in $CDCl_3$.

The copolymers were purified by dissolving in dichloromethane and precipitating in hexane 3 times. The number average molecular weight and molecular weight distribution were determined with GPC using dimethylacetamide (DMAc) as a mobile phase.

^{1}H NMR ($CDCl_3$, 300 MHz) ppm: 5.3 (d, 1H, -C=C**H**-, olefin group in cholesterol), 4.5 (m, 1H, -COO-C**H**-),2.3 (d, 2H, -CH-C**H**$_2$-),0.93 (d, 3H, -CH-C**H**$_3$), 0.88−0.84 (q, 6H, -CH (C**H**$_3$)$_2$), 0.68 (s, 3H, -C-C**H**$_3$). 1.76 (s, 2H, -**CH$_2$**-C(CH_3)COO-), 0.89-0.73 (s, 3H, -CH_2 C**(CH$_3$)**COO-)), 4.01 (t, 2H, -COO-**CH$_2$**-), 3.50-3.27 (t, 6H, -**CH$_2$**-N(COO(CH_3)$_3$- **CH$_2$-CH$_2$** NH(COO(CH_3)$_3$), 1.45-1.42 (s, 18H -N(COO-**(CH$_3$)$_3$**)-CH_2-CH_2-NH- (COO**(CH$_3$)$_3$**), 4.98-4.77 (s, 1H, -CH_2-**NH**-(COO(CH_3)$_3$).

The amino groups of copolymers were deprotected. In order to remove Boc groups, 4.35 μmol Boc-AEAEMA part of the copolymers was dissolved in 1 ml DCM. Trifluoroacetic acid (0.5 ml) dropped into the solution at 0^0 C and the reaction solution was stirred for 30 min at room temperature. The solvent was then removed by purging N_2. Finally, the reaction mixture was then washed with diethyl ether and chloroform more than three times and the sample was dried in a vacuum oven.

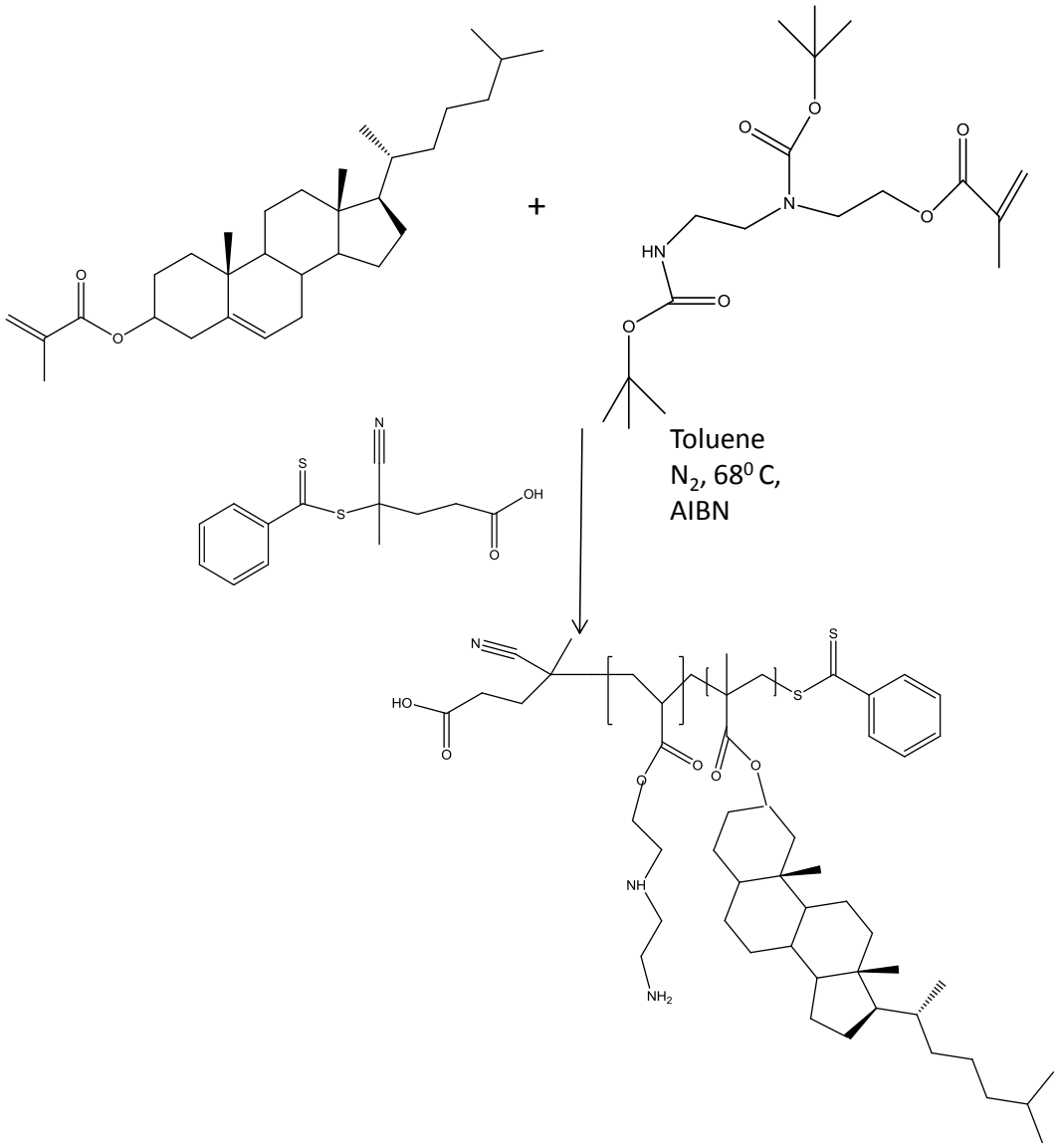

Figure 3.5. Synthesis of p(CMA-co-Boc-AEAEMA)

Table 3.2. Conditions for copolymerization of CMA and (Boc-AEAEMA). Cholesteryl Methacrylate Monomer (CMA), 2-((tert-butoxycarbony) (2-((tert-butoxy carbonyl) amino) ethyl) amino) ethyl Methacrylate monomer (Boc-AEAEMA), initiator (AIBN) and RAFT agent (4-Cyano-4-(phenylcarbonothioylthio) pentanoic acid).

Total Monomer Concentration (M)	[Boc-AEAEMA]/[CMA]/[RAFT]/[AIBN] Mole Ratio	Polymerization Time (h)
1.5	22.5/2.5/1.0/0.2	2,4,6,8
1.5	20.0/5.0/1.0/0.2	2,4,6,8
1.5	15.0/10.0/1.0/0.2	2,4,6,8

3.3.5. Determination of pH-Responsive Behavior of P(CMA-co-MAA)

The turbidity change of polymer solutions at varying pH values was investigated via UV−visible spectroscopy to determine pH-responsive behavior of polymers. Phosphate and citrate buffer solutions at two different pH values (5.5 and 7.4) were prepared. Citrate buffer solution (150 mM) at pH 5.5 was prepared by mixing citric acid (0.1 M) and dibasic sodium phosphate (0.2 M) aqueous solutions. Phosphate buffer solution (150 mM) at pH 7.4 was prepared by mixing sodium phosphate monobasic (0.1 M) and sodium phosphate dibasic (0.1 M) aqueous solutions. The ionic strengths of the buffer solutions were adjusted to 0.15 M by the addition of NaCl to yield isotonic solutions. Copolymers having 2% or 8% CMA content were dissolved in buffer solutionsat a concentation of 0.125 mM.

Dynamic light scattering studies were performed using a Malvern Zetasizer NaNo ZS Instrument (Malvern, U.S.A.). The polymer aqueous solutions (0.125 mM) were prepared at two different pH values (pH 5.5 and 7.4). Measurements were repeated three times.

The absorbance of each polymer solution from acidic pH to neutral (pH 5.5 and 7.4) was measured using an UV−visible spectrophotometer (Thermo Fisher) at 500 nm. Quartz cuvettes were used. Measuerements were repeated three times.

3.3.6. Determination of Hemolytic Activity of Polymers

pH-dependent membrane-disruption activity of polymers on red blood cells was tested via hemolysis assay (Murthy et al., 1999). Briefly, red blood cells were washed with 150 mM saline, and then suspended in 100 mM phosphate buffer solution at pH 5.5 or pH 7.4. The cell suspensions were then diluted to a concentration of 10^8 cell /200 µl using relevant buffer solution. 200 µl of cell solution was taken and mixed with 800 µl of polymer solution dissolved in pH 5.0 or pH 7.4 buffer solution at the desired concentration. The final solutions were incubated at 37 °C for one hour. After incubation period, solutions were centrifuged to remove cell debris and supernatants were transferred to a 96-well plate for absorbance measurements at 541 nm. Cell solutions treated with triton X-100 solution and phosphate buffer solution were used as positive and negative controls, respectively. Experiments were performed in triplicate.

3.3.7. Determination of *In Vitro* Cytotoxicity

In cytotoxicity analysis, NIH 3T3 cells were seeded a day before to polymer sample exposure at 10,000 cells per well (96 well plate) in culture medium containing 10% FBS/DMEM. Polymer sample stocks were prepared in PBS solution. 5 µl of polymer solution was added at predetermined concentrations to cells. The cells were incubated at 37 °C/5% CO2 for 24 or 72 h. The culture medium was removed from the wells after the incubation period. The solution of 3-(4,5-dimethylthiazol-2-yl)-2,5-diphenyl tetrazolium bromide (MTT) dye was prepared with culture medium (10 % v/v). MTT solution (100 µl) was added to wells according to manufacturer's protocol. The plates were incubated at 37 °C for another 4 h and metabolic activity was detected by spectrophotometric analysis. The absorbance of the solutions was recorded at 540 nm. The cell viability (%) was calculated relative to the positive control (cells not treated with polymers) according to Equation 3.8 in which Acell+sample is the

absorbance of polymer treated cells and Apositive control is the absorbance of untreated cells.

$$\text{Cell Viability (\%)} = \frac{\text{Acell + sample}}{\text{A positive control}} \text{x100} \qquad (3.2)$$

3.3.8. Fluorescent Dye Labelling

The carboxylic acid groups of p(CMA-co-MAA) were first converted to thiol groups. 2 mol% of the carboxylic acid groups was intended to be converted to thiol groups. For this purpose, 20 mg p(CMA-co-MAA) (obtained using [MAA] / [CMA] / [RAFT] / [AIBN] mole ratio 490/10/1/0.2; Mn 18200 and 52100; 1.30 and 1.10 PDI; 1.9 and 1.7 CMA content mol %, respectively) ($4.2x10^{-6}$ mole) targeted 2 % methacrylic acid part of the copolymers wasreacted with - N-hydroxysulfosuccinimide (Sulfo-NHS) ($4.2x10^{-6}$ mole) and 1-ethyl-3-(3 dimethylaminopropil)carbodiimide (EDC) ($4.2x10^{-6}$ mole) in pH 5.5 buffer solution (1 ml) for 10 min. Cysteaminium chloride ($8.4x10^{-6}$ mole) was added into the polymer solution. After 3 h of reaction at room temperature, the reaction solution was placed in a dialysis membrane (MWCO: 1000). The dialysis was performed for 3 days against ultra-pure water. The final product was obtained as a white powder from freeze-dryer.

The second step was to conjugate a fluorescence dye to thiol-functionalized copolymers. Oregon Green Maleimide fluorescence dye ($8.4x10^{-6}$ mole) was first dissolved in DMF (50 µl). Separately thiol-functionalized copolymer was dissolved in water (50 µl). Tris(2-carboxyethyl)phosphine (TCEP) (2.8x10^-6 mole) was added into polymer solution. After 5 min reaction, dye solution was added dropwise. The reaction solution was purged with N_2 atmosphere. The reaction was continued for 2 hours at room temperature. Following the addition of fresh TCEP ($1.4x10^{-6}$ mole), the reaction was further carried out for12 hours at room temperature. The final solution was placed in a dialysis tubing (MWCO:1000). The dialysis was performed for 3 days against ultra-pure water at dark medium. The final product was obtained as a white powder from freeze dryer.

3.3.9. Determination of Intracellular Distribution

Intracellular distribution of fluorescent-labelled P(MAA-co-CMA) (2 mol % CMA 20kDA and 60 kDa) was determined via fluorescence microscopy by using DAPI (4', 6-Diamidino-2-Phenylindole, Dilactate)as a nucleus-specific dye. Briefly, NIH3T3 cell was grown on coverslips inside 8 well- plates a day prior to sample exposure at a concentration of 3.5x10^4 cells/well and incubated overnight at 37 °C and 5% CO2 in a humidified atmosphere. Polymers were dissolved in ultrapure water and 50 μM polymer solutions were transferred to wells. The ultra-pure water content of each well was adjusted to be 0.5% (v/v). The final volume of each well was 0.5 ml. The cells were incubated at 37 °C for 1 h and each experiment performed in triplicate.At the end of the incubation period, medium was removed and wells were washed with PBS three times and cells were fixed by using 2% paraformaldehyde containing PBS for 10 minutes at 37^0 C. Wells were washed with PBS three times to remove excess fixation solution. The stock DAPI solution was diluted to 150 nM and 500 μl of the diluted solution was transferred onto coverslips. After the incubation for 5 minutes at dark, the wells were rinsed with PBS three times and excess buffer was drained from coverslip. Coverslips were mounted and necessary microscopy settings were applied. The excitation and emission wavelengths were 496-524 nm and 358-461 nm for Oregon Green Maleimide 488® and DAPI, respectively.

CHAPTER 4

RESULTS AND DISCUSSION

4.1. Synthesis of Cholesteryl Methacrylate

In this study the first step was to synthesize cholesteryl methacrylate monomer. The synthesis procedure was carried out according to previous report (Sevimli, Inci et al. 2012) ^{1}H-NMR spectrum of the synthesized monomer is shown in Figure 4.1. Methacrylate signals were clearly observed at 5.58, 6.08 and 1.93 ppm (Figure 4.1, CH_2, r and q, and CH_3 d). The spectrum indicated that the desired product at high purity (approximately 100%) was obtained.

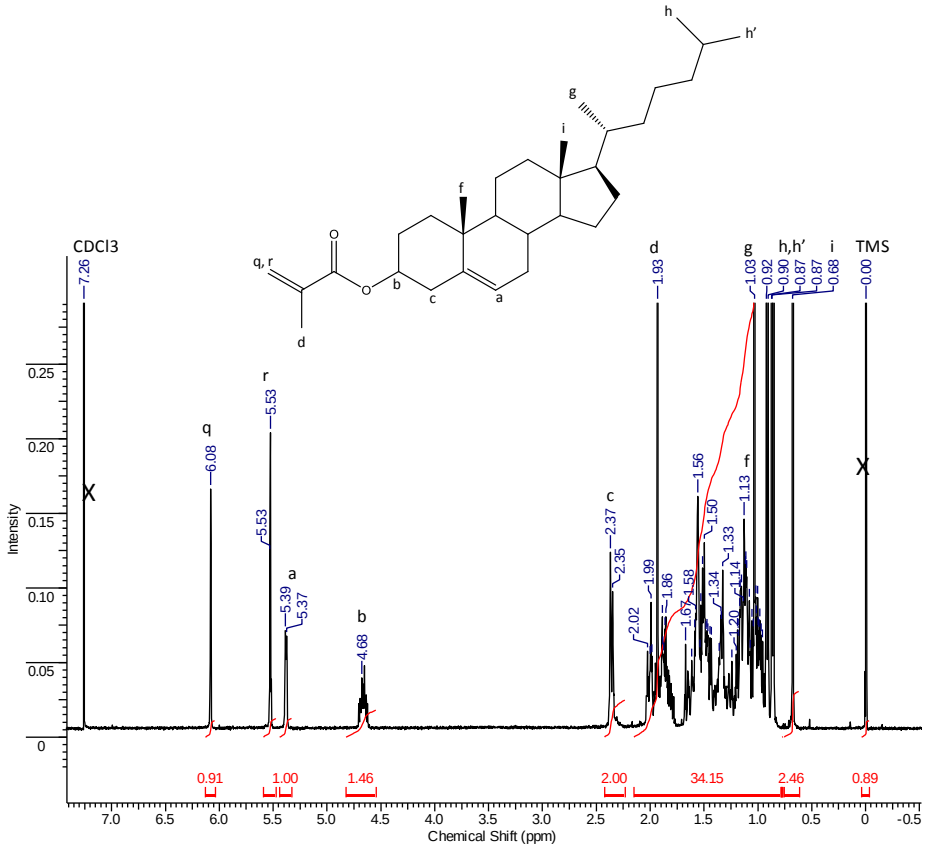

Figure 4.1. ^{1}H-NMR spectrum of cholesteryl methacrylate monomer

4.2. Synthesis of 2-((Tert-butoxycarbony)(2-((tert-butoxycarbonyl) amino) ethyl) amino) ethyl Methacrylate

An amine-containing monomer was also synthesized in this study. The synthetic procedure was adapted from Kurtulus et al. (Kurtulus, Yilmaz et al., 2014). The monomer was synthesized to contain di-*tert*-butyl dicarbonate- (Boc-) protected primary and secondary amine groupsto prevent any possible unwanted side reactions such as aminolysis of the RAFT agent during RAFT polymerization.

^{1}H-NMR spectrum of this monomeris shown in Figure 4.2. The characteristic signals of vinyl protons were observed at 1.93, 5.57 and 6.10 ppm (-C**H$_3$,** 3H, **f,** and –C**H$_2$, 2H e and d)**. Upon methacrylation of Boc-protected ethylenediamine, the signal of - CH2- group (**b**) adjacent to ester bond shifted to 4.24-4.23 ppm, as expected. The signals at 1.44-1.41 ppm belong to Boc- group methyl protons (**a**).

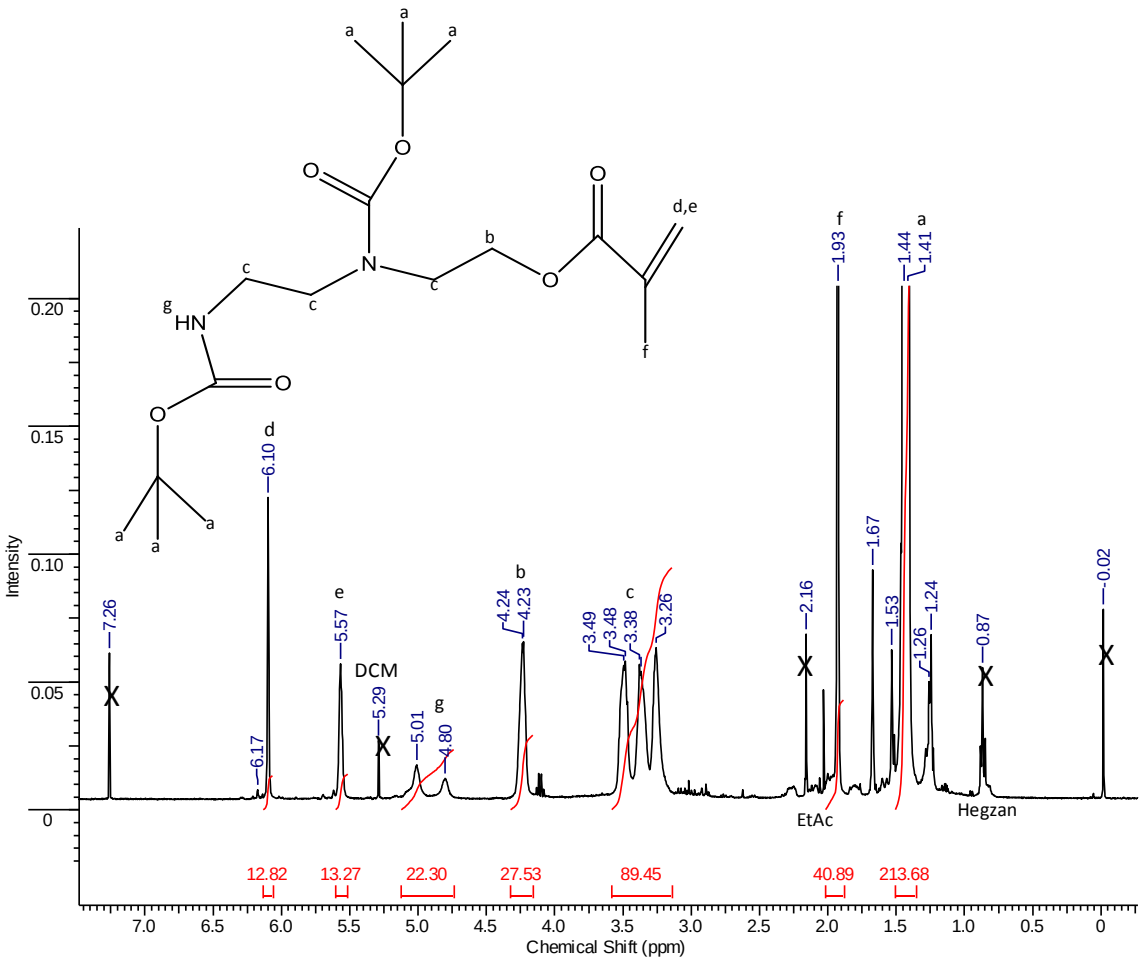

Figure 4.2. ^{1}H-NMR spectrum of monomer 2-((tert-butoxycarbony)(2-((tert-butoxycarbonyl) amino) ethyl) amino) ethyl methacrylate

4.3. RAFT Copolymerization of Cholesteryl Methacrylate and t-Butyl Methacrylate

To make cholesterol-co-methacrylic acid copolymers, cholesteryl methacrylate (CMA) and t-butyl methacrylate (t-BMA) were first copolymerized via Reversible Addition Fragmentation Chain Transfer (RAFT) polymerization. The copolymerization procedure was adapted from Sevimli et al. (Sevimli, Inci et al. 2012). Since methacrylic acid and CMA are not soluble in a common solvent because of significantly different polarity, CMA was copolymerized with t-BMA, followed by the hydrolysis of t-butyl esters to methacrylic acid (MAA) units. Sevimli et al. previously synthesized t-BMA-*co*-CMA copolymers having molecular weights ranging between 15 kDa and 20 kDa. In this previous study, copolymers of MAA-co-CMA that were obtained after hydrolysis of t-BMA units were water soluble only when copolymers had a CMA content less or equal to 8mol%. In this current study, higher molecular weight copolymers (>15,000 and <100,000 g/mol) with varying CMA content were intended to be synthesized to investigate whether higher molecular weight p(MAA-co-CMA) having CMA content more than 8% is more water-soluble or -dispersible and can interact with cellular membranes more efficiently.

Briefly, copolymerization of CMA and t-BMA was performed in toluene as an organic solvent. A well-kown azo initiator, AIBN was used as a polymerization initiator. 4-cyano-4-(phenylcarbonothioylthio) pentanoic acid was used as the chain transfer (RAFT) agent. Firstly, polymerization kinetics and RAFT-controlled mechanism were investigated at two different total monomer concentrations (4.2 and 5.9 M) and a constant [t-BMA]/[CMA]/[RAFT]/[Initiator] mole ratio of 490/10/1.0/0.2. Figure 4.3. shows the plots of $\ln([M]_0/[M])$ versus polymerization time. Pseudo-first order kinetics were observed at both monomer concentrations, indicating constant radical concentration during polymerizations, which is characteristic to RAFT-controlled polymerization mechanism. Figure 4.3, shows the plots of number average molecular weight (M_n) and polydispersity (PDI) of the resulting polymers versus monomer conversion. The M_n values increased linearly with monomer conversion, while low polydispersities (mostly <1.2) were maintained throughout polymerizations. These are all known traits of RAFT-controlled polymerizations.

According to the results of polymerization kinetics, an initial monomer concentration of 4.2 M and a [Monomer]/[RAFT]/[Initiator] mole ratio of 500/1/0.2

yielded polymers in the desired molecular weight range. Accordingly using the same polymerization parameters and varying initial comonomer concentrations (t-BMA/CMA = 490/10; 480/20, 460/40, 450/50) large scale polymer syntheses were performed to produce polymers with varying molecular weights and compositions. The result of large scale-polymerizations is presented in Table 4.1. The results show that well-defined p(t-BMA-*co*-CMA) copolymers having molecular weights ranging between 2 kg/mol and 90 kg/mol and CMA contents between 2 mol% and 10 mol% could be synthesized. The conversion of monomer was calculated from ^{1}H-NMR of crude polymer in Appendix-A using the Eq 4.1.

$$\text{Monomer conversion } \% = \frac{\left[\left(\frac{a+b}{2}\right)-\left(\frac{q+r}{2}\right)\right]+\left[\left(\frac{m+z}{9}\right)-\left(\frac{j+k}{2}\right)\right]}{\left(\frac{a+b}{2}\right)+\left(\frac{m+z}{9}\right)} x100 \qquad (4.1)$$

Table 4.1. Lists of the number average molecular weights (Mn's), molecular weight distributions (PDI's) and the composition of poly (cholesteryl methacrylate-co-t-butyl methacrylate) p(CMA-co-t-BMA) synthesized throughout the study.

	Total Monomer Concentration (M)	[t-BMA]/[CMA]/[RAFT]/[AIBN]	Time (h)	Mn (g/mol)	PDI	CMA % in the copolymer	t-BMA % in the copolymer
20K	4.2	490/10/1/0.2	3	18200	1.30	1.9	98.1
30K	4.2	490/10/1/0.2	8	29000	1.12	1.7	98.3
40K	4.2	490/10/1/0.2	7	42000	1.08	1.6	98.4
50K	4.2	490/10/1/0.2	13	52100	1.10	1.7	98.3
60K	4.2	490/10/1/0.2	18	57200	1.12	1.4	98.6
4K	4.2	480/20/1/0.2	6	3760	1.52	3.7	96.3
12K	4.2	480/20/1/0.2	8	12000	1.18	3.6	96.4
30K	4.2	480/20/1/0.2	18	35000	1.19	4.1	95.9
20K	4.2	460/40/1/0.2	8	16800	1.01	7.3	92.7
30K	4.2	460/40/1/0.2	6	27000	1.18	8.2	91.8
70K	4.2	460/40/1/0.2	18	66100	1.48	8.2	91.8

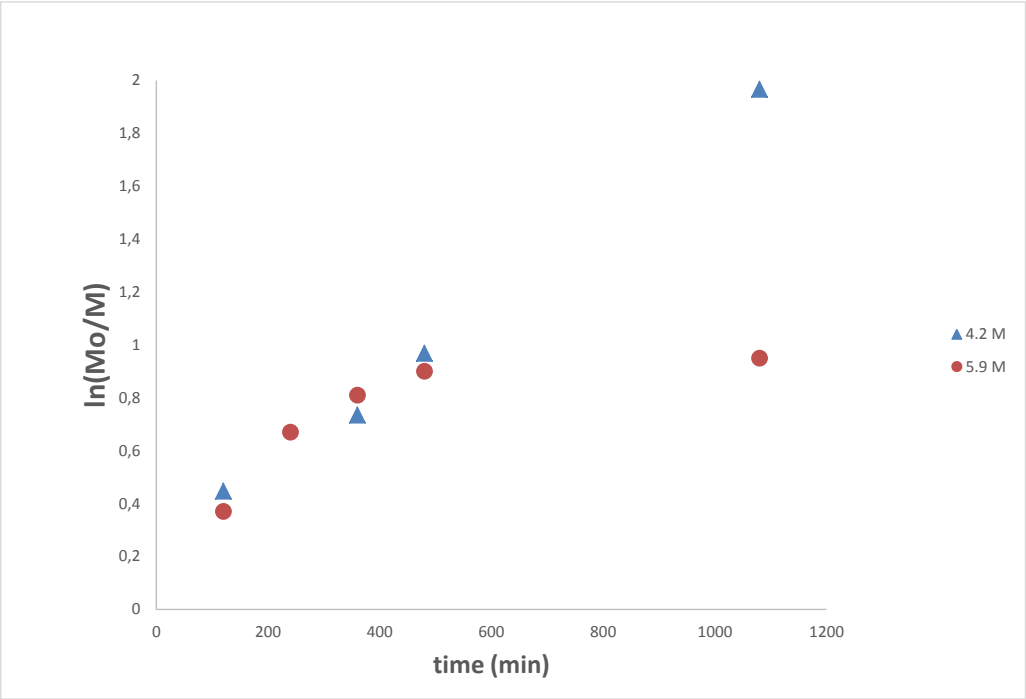

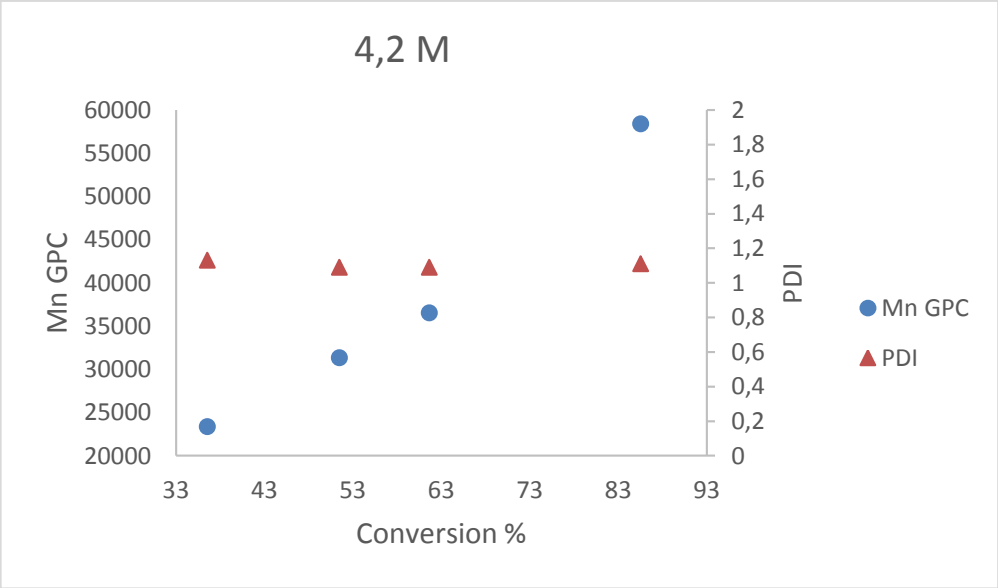

Figure 4.3. Methacrylate at total monomer concentrations of 4.2 M (blue) and 5.9 M (red).[t-BMA]/[CMA]/[RAFT]/[AIBN]= 490/10/ 1/ 0.2. A) Ln $[M]_0/[M]$ versus polymerization time; B) Mn and PDI versus monomer conversion. Mo and M are the monomer concentrations in the initial polymerization feed and left after polymerization, respectively.

(Cont. on next page)

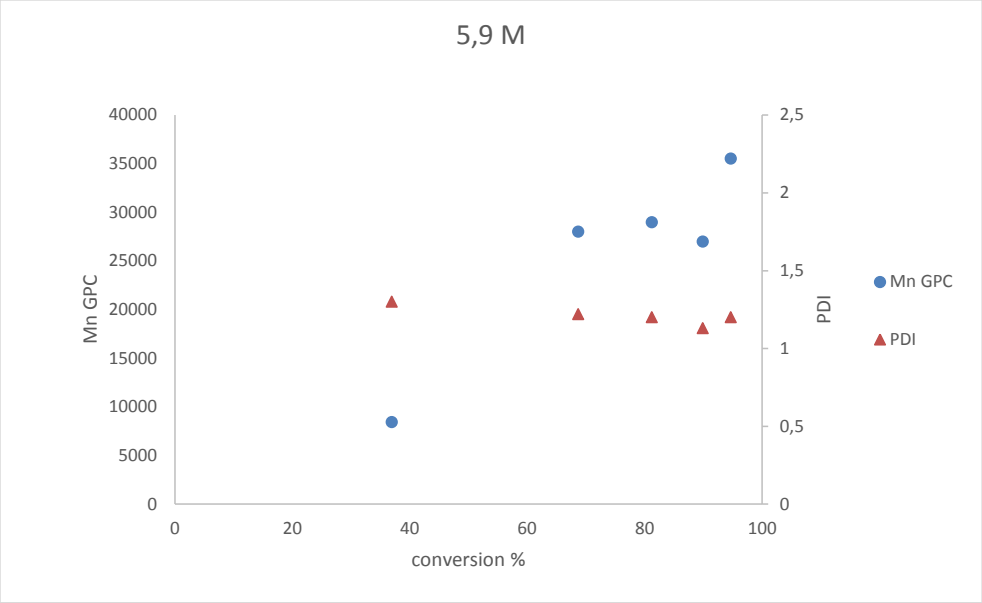

Fig 4.3. (cont.)

In order to obtain soluble copolymers in water, p(t-BMA-co-CMA) was hydrolyzed to p(CMA-co-MAA) in the presence of trifluoroacetic acid.[1]H-NMR spectra of p(CMA-co-t-BMA) and p(CMA-co-MAA) copolymers after purifications are given in Figure 4.4. As seen in the spectra, t-butyl group (**z) does** not exist after hydrolysis and the signal of methacrylic acid proton (COO**H**) exists in the spectrum of copolymer after hydrolysis. The polymer backbone before and after hydrolysis did not show any differences as calculated using Eq. 4.1, indicating that the acid hydrolysis did not alter the copolymer structure except the t-BMA units. After hydrolysis of copolymers with varying molecular weights and CMA contents, it was observed that only copolymers with 2 and 4% CMA content became water soluble and the copolymer with 8% CMA were partially water-soluble, regardless of molecular weight The copolymer having 10 % CMA was not soluble in water due to the highly nonpolar nature of cholesteryl methacrylate units.

$$\frac{\int \text{backbone}}{\int \text{a}} = \frac{\int \text{v} - (\int \text{ax46}) - (\int \text{m} + \int \text{z})}{\int \text{a}}$$

$$\frac{\int backbone}{\int a} = \frac{\int v - (\int ax46)}{\int a} \qquad (4.2)$$

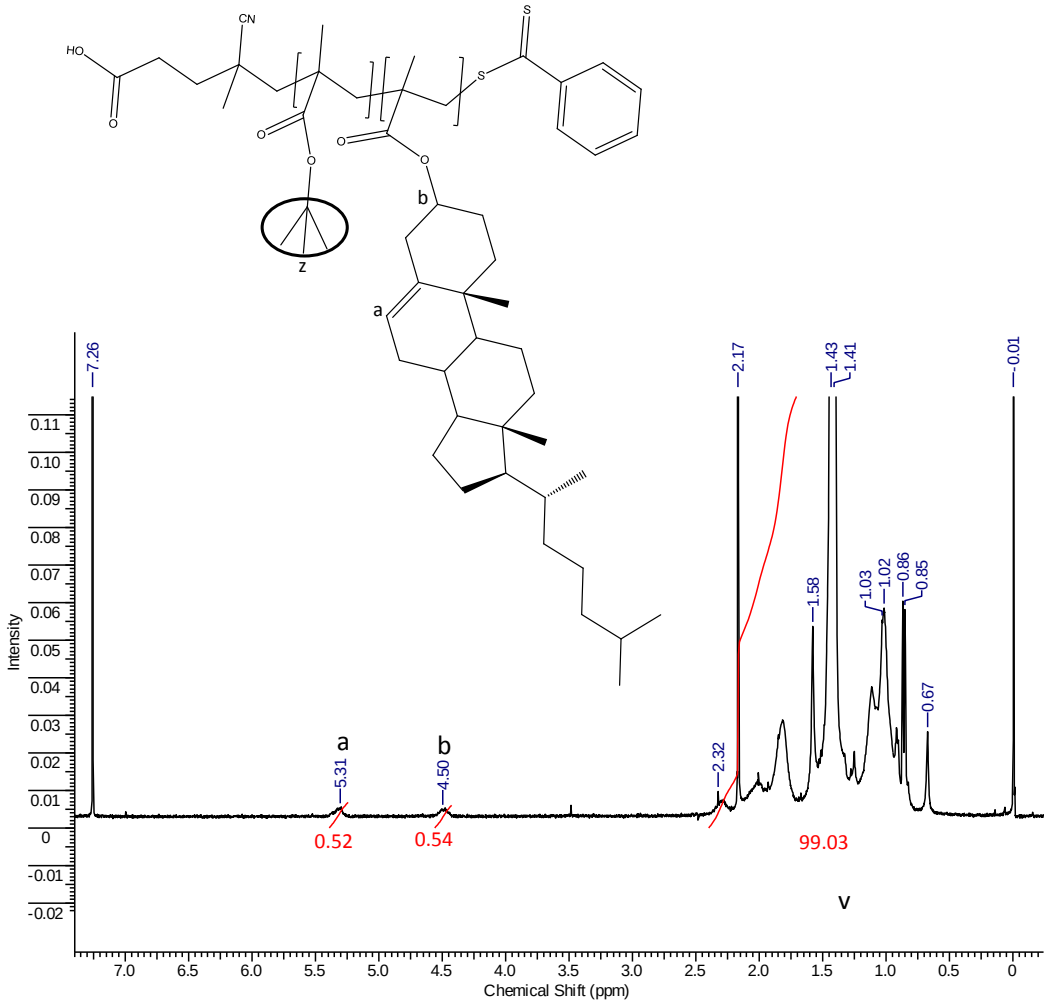

Figure 4.4. ^{1}H-NMR spectra of P(t-BMA-co-CMA) (A) before and (B) after hydrolysis ([Total Monomer]= 4.2 M; [t-BMA]/[CMA]/[RAFT]/[AIBN] mole ratio= 450/50/1/0.2; Mn = 89517 g/mol; CMA= 10.4%) Spectra before and after hydrolysis are in $CDCl_3$ and DMSO-d_6, respectively. 90K polymer (Tot.Mon.Conc.=4.2M; [t-BMA]/[CMA]/[RAFT]/[AIBN] Mole ratio= 450/50/1/0.2 ; Mn (g/mol)= 89517) ^{1}H-NMR spectrum in DMSO-d_6 after hydrolysis (bottom).

(Cont. on next page)

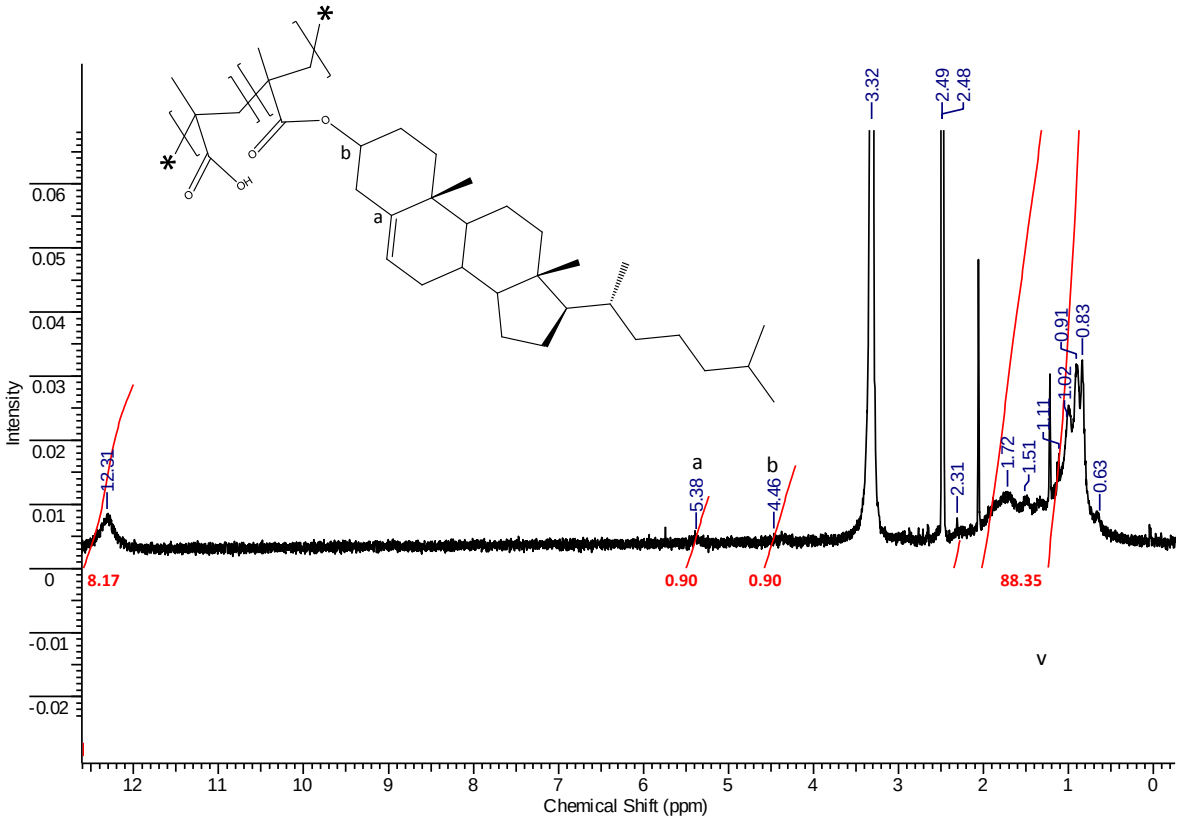

Fig 4.4. (cont.)

4.4. RAFT Copolymerization of Cholesteryl Methacrylate and 2-((Tert-butoxycarbony)(2-((tert-butoxycarbonyl)amino)ethyl)amino)ethyl Methacrylate

Cholesteryl Methacrylate was also copolymerized with a cationic monomer, 2-((tert-butoxycarbony)(2-((tert-butoxycarbonyl) amino)ethyl)amino)ethyl methacrylate to produce amphiphilic cationic copolymers as potential endosomal escaping agents. The polymerization was performed via RAFT polymerization using 4-cyano-4-(phenylcarbonothioylthio) pentanoic acid as a RAFT agent. The RAFT copolymerization of CMA and Boc-AEAEMA was performed in toluene.AIBN was used as the polymerization initiator. RAFT polymerization kinetic was investigated at a [Total Monomer]/ [RAFT agent]/[Initiator] ([M]/[R]/[I]) ratio of 25/1/0.25 and varying [Boc-AEAEMA]/[CMA] ratios (22.5/2.5, 20/5, 10/15) The total monomer

concentration was 1.5 M. Figure A2. in Appendix shows representative ^{1}H NMR spectra of a polymerization mixture and purified copolymer. Figure 4.5, Figure 4.6 and Figure 4.7 show the plots of ln ($[M]_0/[M]$) versus polymerization time, and Mn and PDI versus monomer conversion.

In all polymerizations, ln [M]0/[M] increased linearly with time, indicating pseudo-first order behavior of polymerization. The linear increase in Mn with monomer conversion and low PDI values were also observed. These are all attributed to the known traits of the RAFT-controlled polymerization mechanism. With the increase in the CMA content in the polymerization feed, an increase in the monomer conversion and a deviation from linearity in all plots was observed. This suggested the partial loss of RAFT controlled mechanism possibly due to the bulk structure of CMA monomer.

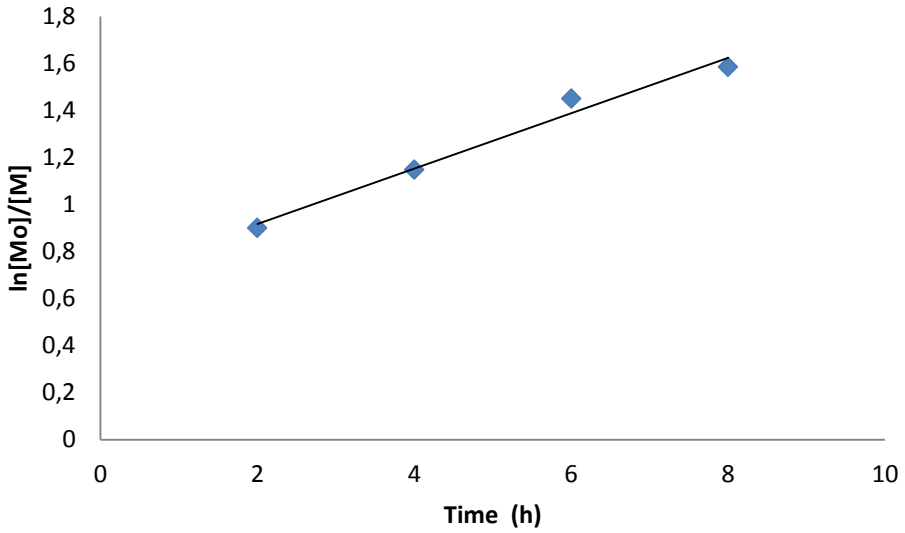

Figure 4.5. Kinetic plots of RAFT copolymerization of p(Boc-AEAEMA-co-CMA). total monomer concentration=1.5M [Boc-AEAEMA]/[CMA]/[RAFT]/[AIBN]= 22.5/2.5/ 1.0/ 0.25). A) Ln [M]0/[M] versus time; B) Mn and PDI versus monomer conversion. Mo and M are the monomer concentration in the initial polymerization feed and left after polymerization, respectively.

(Cont. on next page)

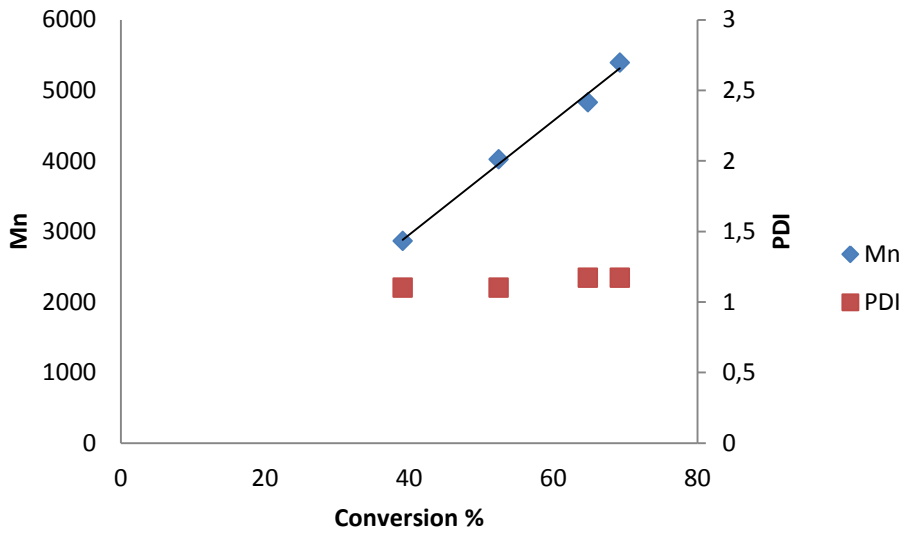

Figure 4.5. (cont.)

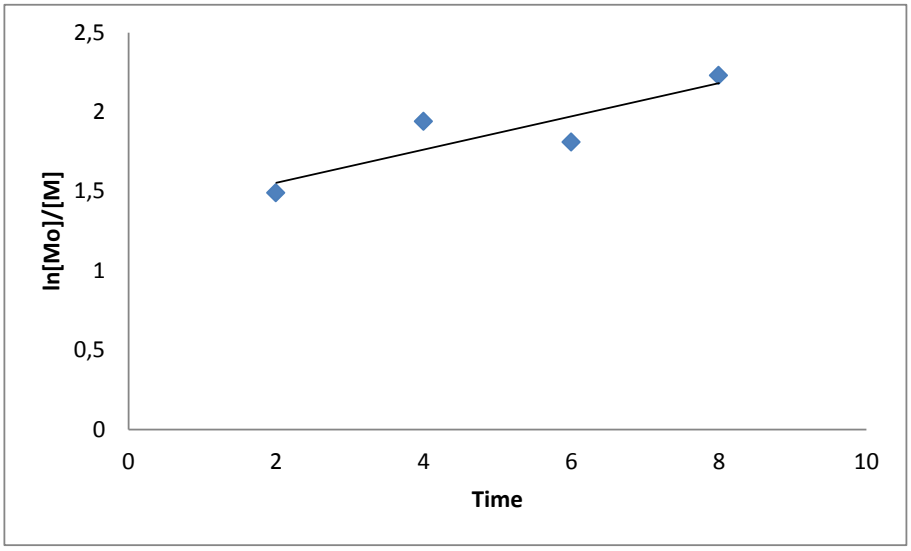

Figure 4.6. Kinetic plots of RAFT copolymerization of poly[2-((Tert-butoxycarbony)(2-((tert-butoxycarbonyl)amino)ethyl)amino)ethyl Methacrylate-co-Cholesteryl Methacrylate] total monomer concentration=1.5M [Boc-AEAEMA] / [CMA] / [RAFT] / [AIBN]= 20.0/5.0/1.0/0.25). A) Ln [M]0/[M] versus time; B) Mn and PDI versus monomer conversion. Mo and M are the monomer concentration in the initial polymerization feed and left after polymerization, respectively.

(Cont. on next page)

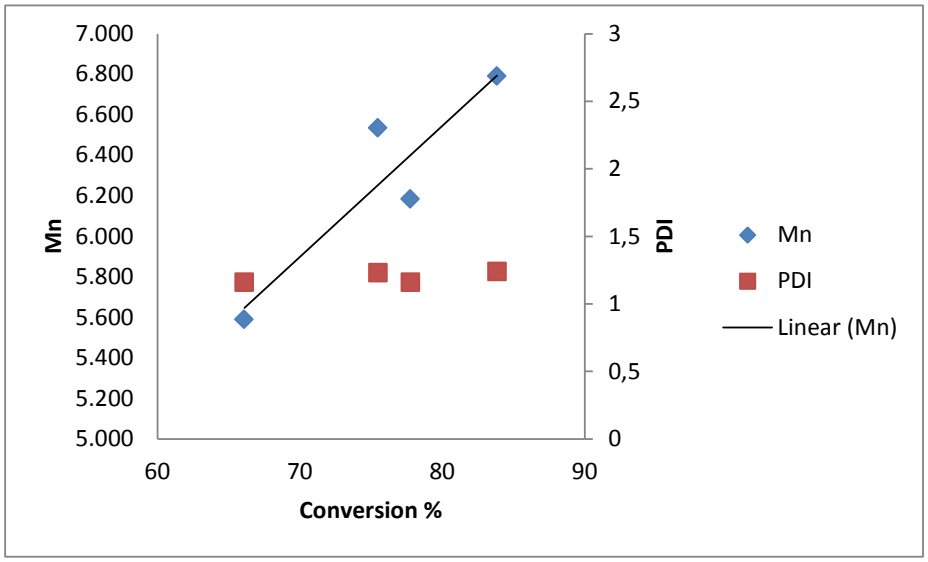

Figure 4.6. (cont.)

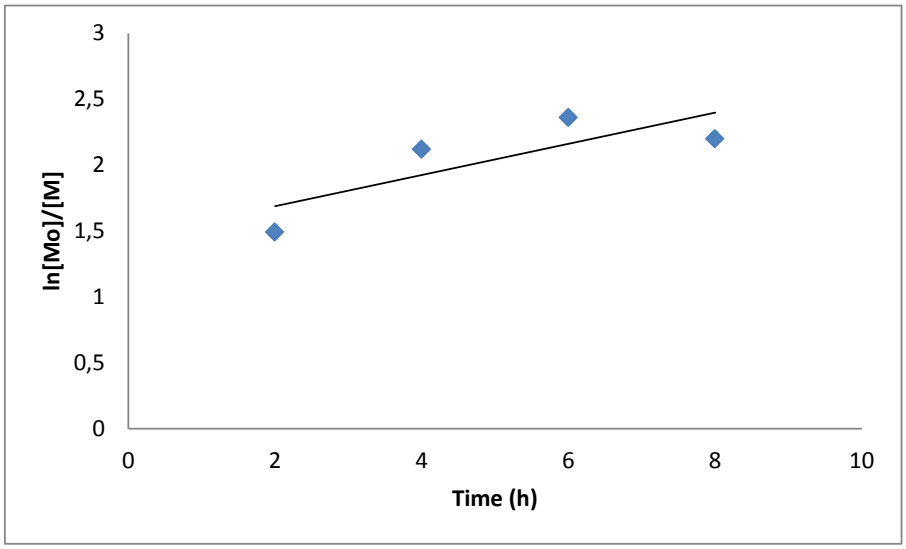

Figure 4.7. Kinetic plots of RAFT copolymerization of poly[2-((Tert-butoxycarbony)(2-((tert-butoxycarbonyl)amino)ethyl)amino)ethyl Methacrylate-co-Cholesteryl Methacrylate] total monomer concentration=1.5M [Boc-AEAEMA]/[CMA]/[RAFT]/[AIBN]= 15/10/ 1/ 0.25). A) Ln [M]0/[M] versus time; B) Mn and PDI versus monomer conversion. Mo and M are the monomer concentration in the initial polymerization feed and left after polymerization, respectively.

(Cont. on next page)

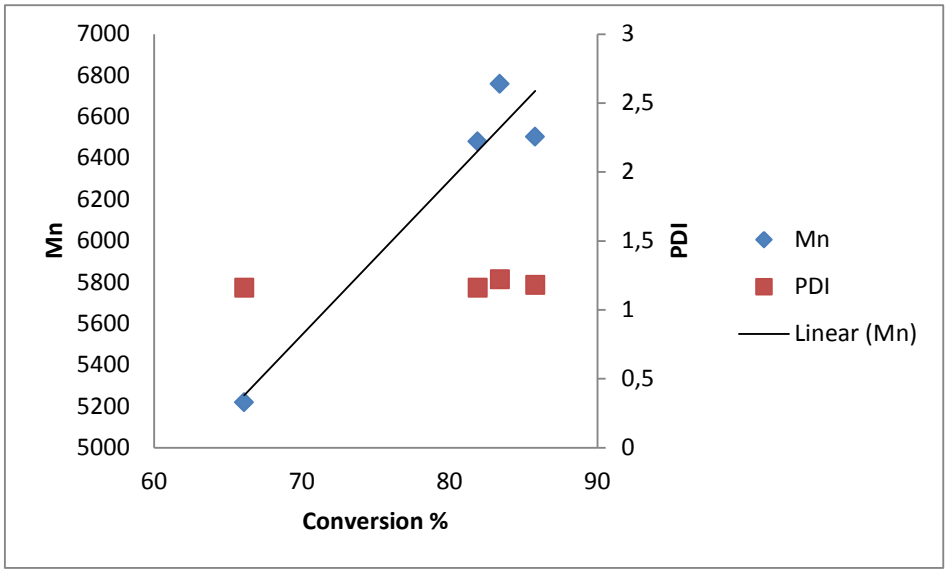

Figure 4.7. (cont.)

After deprotection of amino groups, it was observed that the p(AEAEMA-co-CMA) with 40 % CMA content did not dissolve in water er while the other copolymers (with 10 and 20 mol% CMA content) were completely soluble. Hence combining CMA with cationic monomer yielded copolymers with improved water-solubility property. The investigations on the pH-responsive behavior, cytotoxicity, intracellular distribution and cell membrane interaction of these new copolymers would be the focus of future studies.

4.5. Determination of pH-Responsive Behavior of CMA-co-MAA Copolymers

The pH-responsive behavior of p(MAA-co-CMA) was analyzed via DLS. The hydrodynamic diameter of copolymers having varying molecular weights and 2, 4 or 8 % CMA content was investigated at pH 5.5 and pH 7.4. The final concentration of polymers in buffer solutions was 0.125 mM. The DLS results of copolymer solutions are given in Figure 4.8-Figure 4.10 .

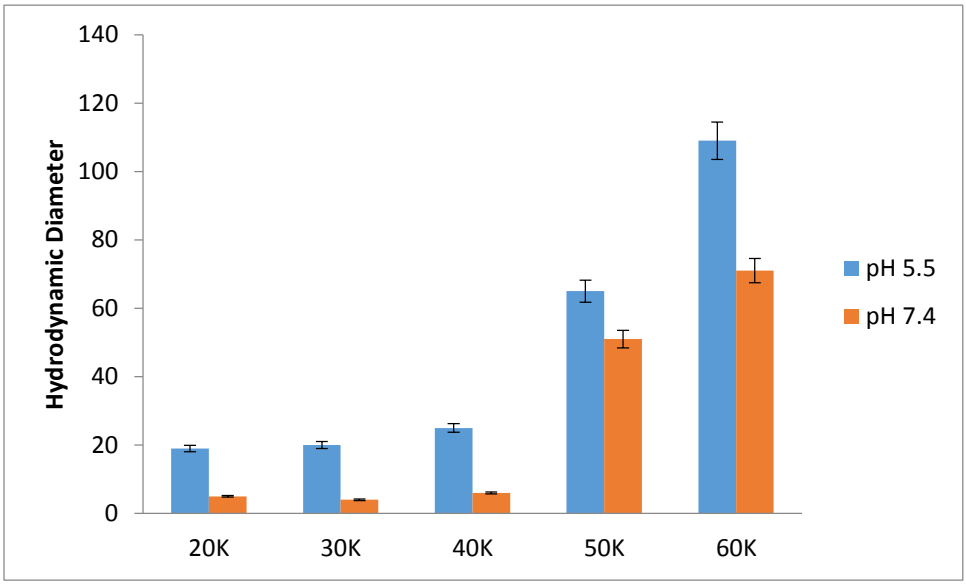

Figure 4.8. DLS results of the copolymers having different molecular weights and 2 mol % CMA content at varying pHs (pH 5.5 and 7.4).

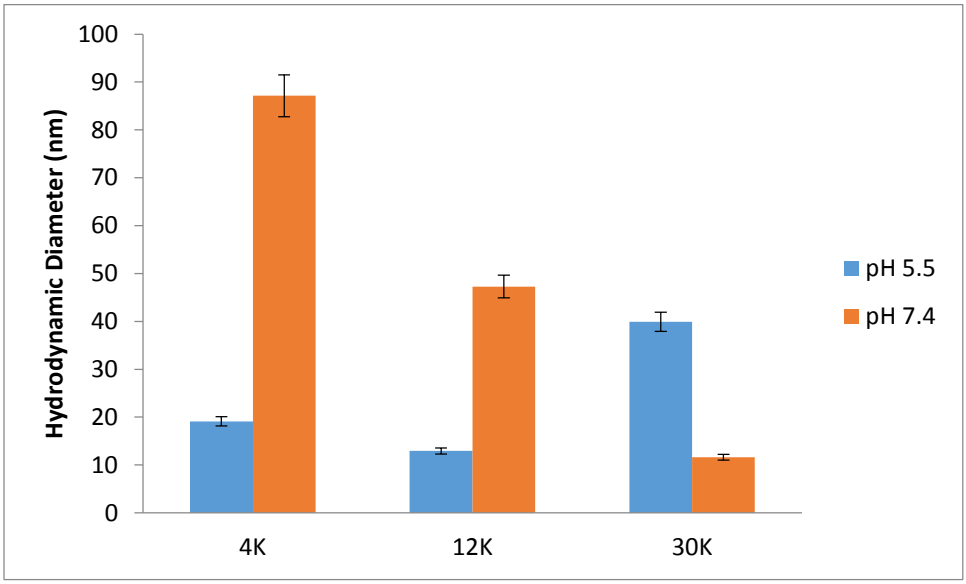

Figure 4.9. DLS results of the copolymers having different molecular weights having 4 mol % CMA content at varying pHs (pH 5.5 and 7.4).

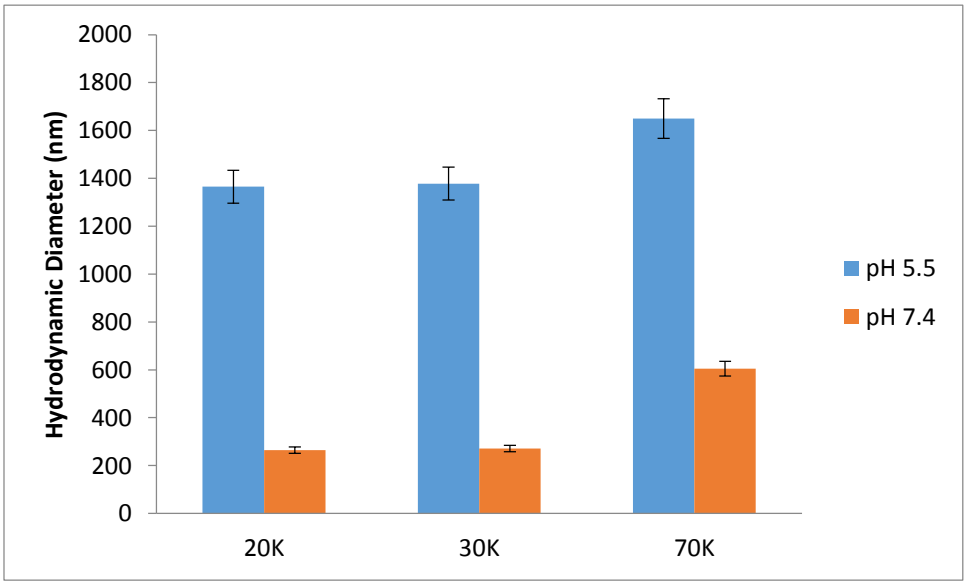

Figure 4.10. DLS results of the copolymers having different molecular weights having 8 mol % CMA content at varying pHs (pH 5.5 and 7.4).

According to DLS results, P(MAA-co-CMA) with 2% CMA exists as unimers in solution at pH 7.4, except the higher molecular weigth ones, i.e. 50 and 60 kDa. However, at pH 5.5 they appear to self-organize in solution to nanoparticles as the hydrodynamic diameters (Dh) are larger than 15 nm. The 2 mol% CMA containing copolymer with the largest molecular weights (50 and 60 kDa) appeared to form nanoparticles at both pH values, indicating enhanced interactions possibly between cholesterol units overcoming the electrostatic repulsions between MAA units at pH 7.4. The copolymers with 8 mol% CMA displayed more significant aggregation tendency, forming particles with D_h above 200 nm at both pH values. Similar to the results of the copolymer with 2 mol% CMA, at pH 7.4, increase in molecular weight of the copolymer having 8 mol% CMA increased the D_h of the particles. At acidic pH, the copolymer with 8 mol% CMA formed giant aggregates regardless of molecular weight, showing enhanced hydrophopic interactions due to the protonation of MAA units.The copolymer having 4 mol% CMA content displayed different pH-responsive behavior, possibly due to relatively small molecular weight range studied with this copolymer. At all pH values, these copolymers appear to exist in a self-organized manner as the Dh values were above 10 nm regardless of pH and molecular weigth, showing the interactions between cholesterol units. Interestingly, the 4% copolymer having lower molecular weights, i.e. 4 and 12 kDa, displayed larger D_h values at pH 7.4 than those at

pH 5.5. This suggests that although MAA units are charged, the interchain interactions between cholesterol units are not disrupted at all, possibly due to the small molecular weigth of the copolymeric chains involved. In other words, the nanoparticles involving a number of copolymeric chains stay intact despite the electrostatic repulsions between MAA units at pH 7.4. The repulsions only increase the D_h value of the nanoparticles when compared with the size of the particles at pH 5.5. At higher molecular weight, i.e. 30 kDa, this behavior become reverse. The interchain interactions between cholesterol units are disrupted at pH 7.4 as the repulsions between negatively charged MAA units along longer polymer chains become dominant, leading to a decrease in D_h of the particles as pH increases from pH 5.5 to pH 7.4.

The pH-responsive phase behaviors of 2% CMA containing copolymers were further investigatedby measuring the turbidity change of polymer solutions at varying pH values via UV−visible spectroscopy Figure 4.11. The final concentration of polymer in buffer solutions was the same with the concentration used in DLS experiment (0.125 mM).

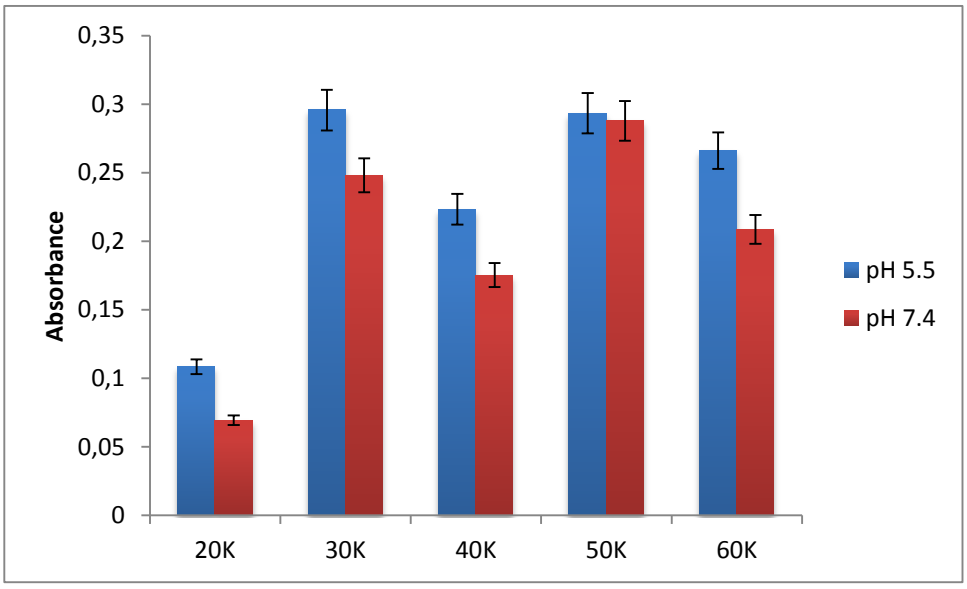

Figure 4.11. Absorbance of copolymer solutions at pH 5.5 or 7.4. Copolymers with 2 mol % CMA and varying molecular weigths were used. Polymer concentration was 0.125 mM.

As seen in Figure 4.11, as molecular weight of copolymers increased, the turbidity of copolymer solution increased. In addition, the turbidity of the copolymers at

acidic pH was slightly higher than that at pH 7.4. These results are in accord with DLS results.

In conclusion, both DLS and UV-Vis spectroscopy result indicated the pH-responsive behavior of copolymers. At acidic pH, copolymers in general (except 4 mol% CMA with lower molecular weights) displayed more hydrophobic character due to the protonation of acidic groups, leading to enhanced hydrophobic interactions and aggregation tendency with increasing molecular weights.

4.6. Determination of *In Vitro* Cytotoxicity

The effect of P(CMA-co-MAA) having 2,4 and 8 mol % CMA on viability of *in vitro* cultured mouse fibroblast NIH 3T3 cell line was investigated using 3-(4,5-dimethyl thiazol-2-yl)-2,5-diphenyl tetrazolium bromide (MTT) cell viability assay.

In the MTT assay, the metabolic activities of living cells reduce tetrazole into purple formazan. The absorbance of purple formazan, which depends on viable cells, was measured using a microplate reader at 540 nm. The percentage of cell viability was determined with respect to untreated cells by Equation 3.2.

According to Figure 4.12-Figure 4.14, the P(MAA-co-CMA) copolymers with different compositions and molecular weights at 250 μg/ml did not show cytotoxic effect.

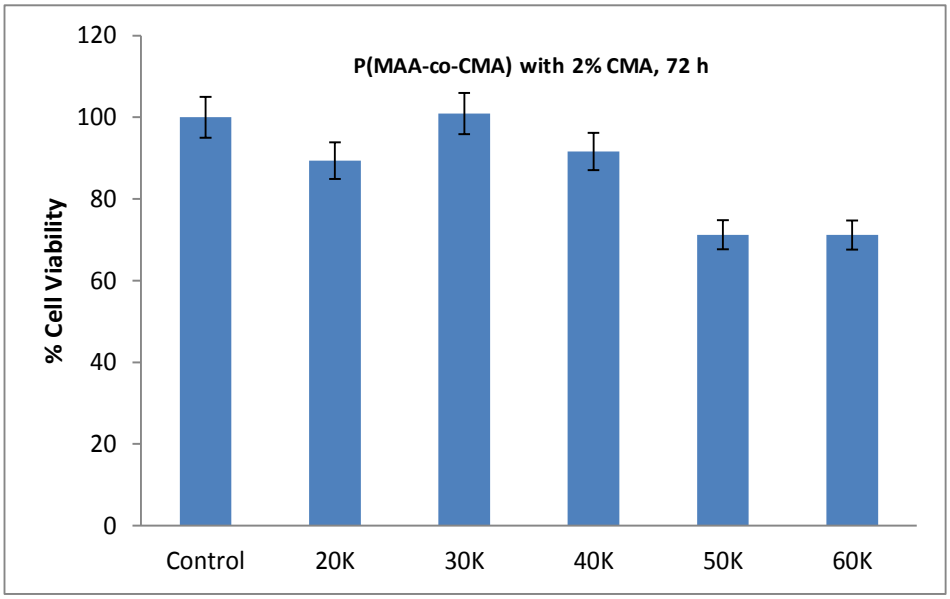

Figure 4.12. Viability of NIH 3T3 cells after incubation with 2% mol CMA content copolymers and for 72 h. Control is the cells with no treatment.

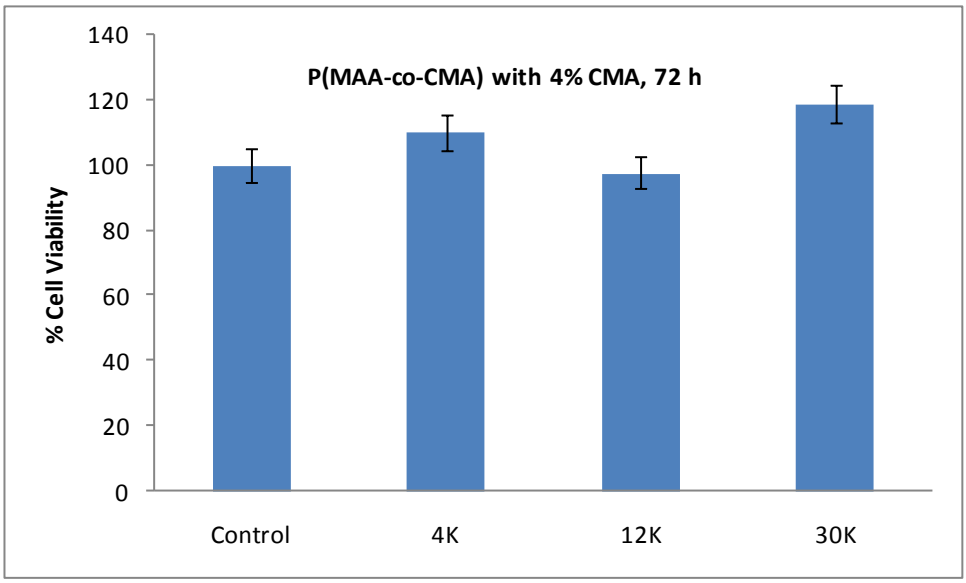

Figure 4.13. Viability of NIH 3T3 cells after incubation with 4% mol CMA content copolymers and for 72 h. Control is the cells with no treatment.

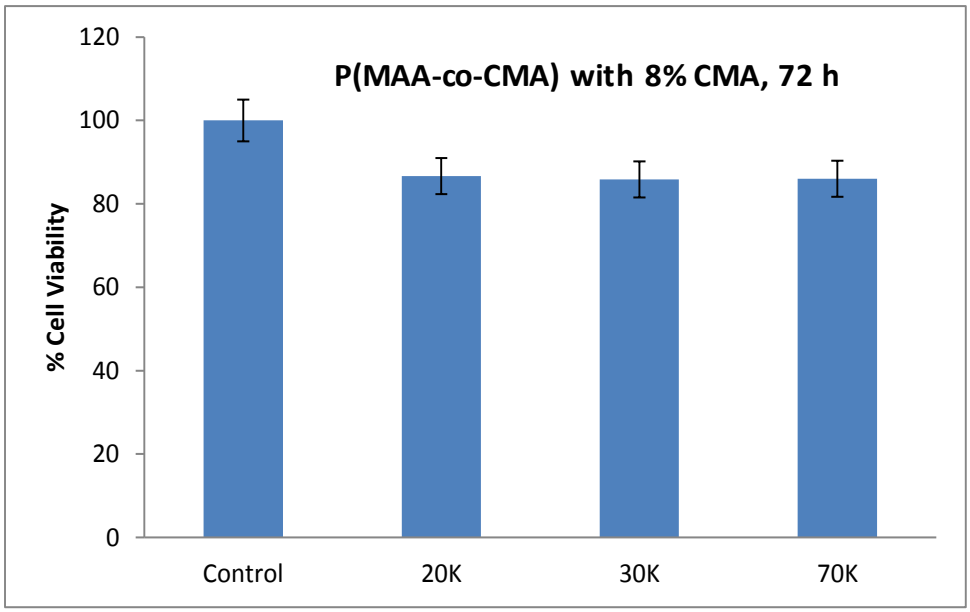

Figure 4.14. Viability of NIH 3T3 cells after incubation with 8% mol CMA content copolymers and for 72 h. Control is the cells with no treatment.

4.7. Hemolytic Activity of Polymers

The hemolytic activity of CMA-co-MAA copolymers having 2, 4 and 8 mol% CMA was evaluated at different pH values (pH 5.5 and pH 7.4) using polymer solutions at 250 μg/ml and 1000 μg/ml. In endocytic pathway, the pH of endosomes gradually decreases. This pH gradient is a key factor in the design of membrane-disruptive polymers which could enhance the endosomal release of drugs. Such polymers are expected to disrupt lipid bilayer membranes at acidic pHs such as 6.0 and lower, but should be non-lytic at pH 7.4. The pH-dependent effect of P(MAA-co-CMA) having a CMA content of 2 , 4 or 8 mol% on the plasma membrane of red blood cells was investigated. Triton X-100 was used as positive control. Experiments were performed in triplicate. The results are shown in Figure 4.15- Figure 4.18.

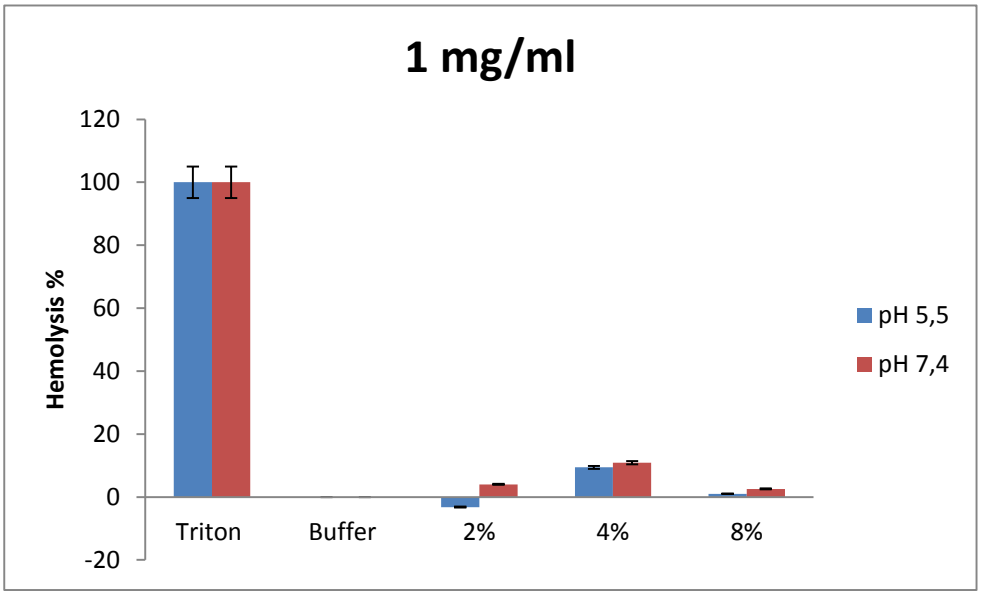

Figure 4.15. The hemolytic activity of P(MAA-co-CMA) with 30 kDa MW and varying compositions (Polymer concentration= 1 mg /ml).

Figure 4.15 shows that copolymers having 30 kDa molecular weight display slightly higher membrane-lytic activity at pH 7.4 when compared with that at pH 5.5, regardless of composition. The hemolytic activity seen in Figure 4.15 supports well the DLS results. Considering both DLS and hemolytic activity results, one can conclude that the deporotonation of MAA units on the copolymer increases the interactions of cholesterol units with the cell membrane despite the negative charge repulsions between membrane and copolymer chains. The enhanced solubility of copolymer chains at pH 7.4 possibly leads to enhanced exposure of cholesterol units and interactions with the cell membrane. The same behavior was observed with copolymer having 2 mol% CMA and varying molecular weigths (Figure 4.16). The copolymer with 8 mol% CMA did not show any activity regardless of pH and molecular weight at the concentration studied, possibly due to strong aggregation behavior. In a similar way, the copolymer having 4 mol% CMA and lower molecular weights (4 and 12 kDa) showed the desired pH-dependent hemolytic activity. When molecular weigth was increased, the hemolytic activity was lost. This result also supports previous finding indicating that the enhanced solubility and decreased aggregation behavior result in enhanced hemolytic activity.

In conclusion, considering both DLS and hemolytic activity results, it is clear that the presence of cholesterol units along the copolymer chain enables the interactions with cell membrane, regardless the amount of cholesterol units, i.e. the presence of a

few cholesterol units is sufficient to provide membrane-activity. However, the intrachain and interchain interactions between cholestrol units, depending on the copolymer concentration in solution, molecular weight of copolymer chains and pH of solution, strongly reduce membrane activity. Higher copolymer concentrations, larger molecular weights (thus more cholesterol units interacting with each other and also a longer hydrophobic backbone contributing to hydrophobic interactions) and acidic pH values (causing protonation of MAA units, hence enhancing the hydrophobicity of the copolymer chains) increase the interactions between cholestrol units and also other hydrophobic interactions, leading to self-organization into particles or aggregation of the copolymers, and decreased hemolytic activity. Hence there should be a delicate balance between all these parameters to obtain the best hemolytic activity of p(MAA-co-CMA).

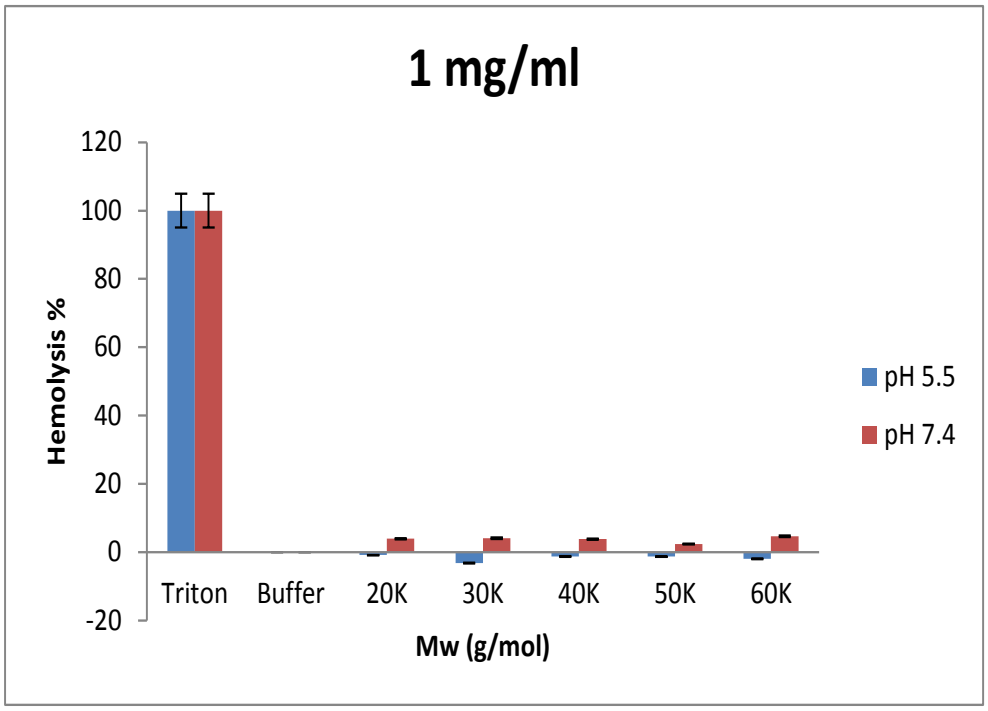

Figure 4.16. The hemolytic activity of P(MAA-co-CMA) with 2% CMA and varying molecular weight (Polymer concentration= 1 mg /ml).

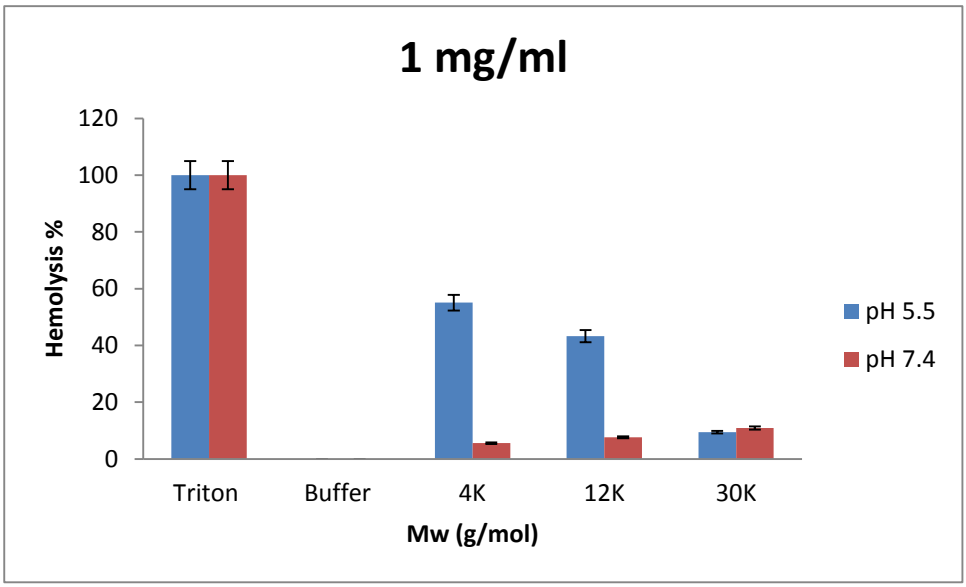

Figure 4.17. The hemolytic activity of P(MAA-co-CMA) with 4% CMA and varying molecular weigth (Polymer concentration= 1 mg /ml).

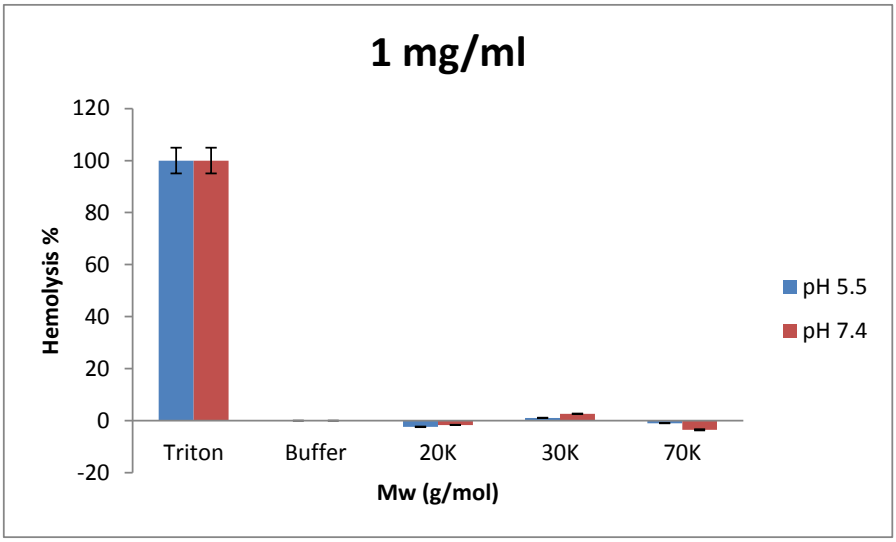

Figure 4.18. The hemolytic activity of P(MAA-co-CMA) with 8% CMA (Polymer concentration= 1 mg /ml).

4.8. Fluorescent Dye Labelling and Intracellular Distribution of Polymers

Labeling of polymers was required for determination of *in vitro* intracellular distribution of polymers. Labeling of polymers is generally based on covalent conjugation of a fluorescent probe to the polymer of interest. Oregon green maleimide®

is one of the green fluorescent probes which can be easily covalently coupled to thiol functionalized polymers (Thiol Reactive Probes Manuel, Molecular Probes- Invitrogen).

The intracellular localization of polymers was determined via fluorescence microscopy. After labeling the polymers with Oregon Green and staining the nucleus selectively with DAPI (4',6-Diamidino-2-Phenylindole Dilactate-a blue fluorescent dye), the images of NIH3T3 cells were obtained. The images of NIH3T3 cells after incubation with polymers are shown in Figure 4.19-Figure 4.20.

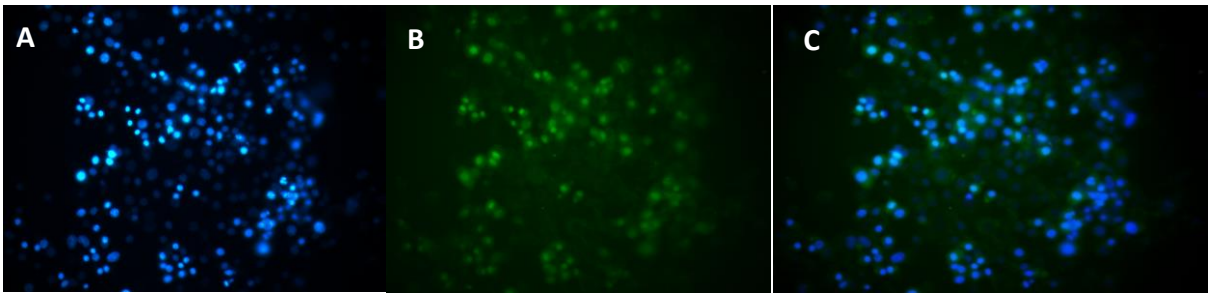

Figure 4.19. Fluorescence micrographs of NIH3T3 cells after incubation with Oregon Green (OG) labeled P(MAA-co-CMA) with 2 % CMA (Mw: 20 kDa) at 40X magnification a)Nucleus staining by DAPI b) Incubation with OG-labeled Copolymer c) Merge of a and b.

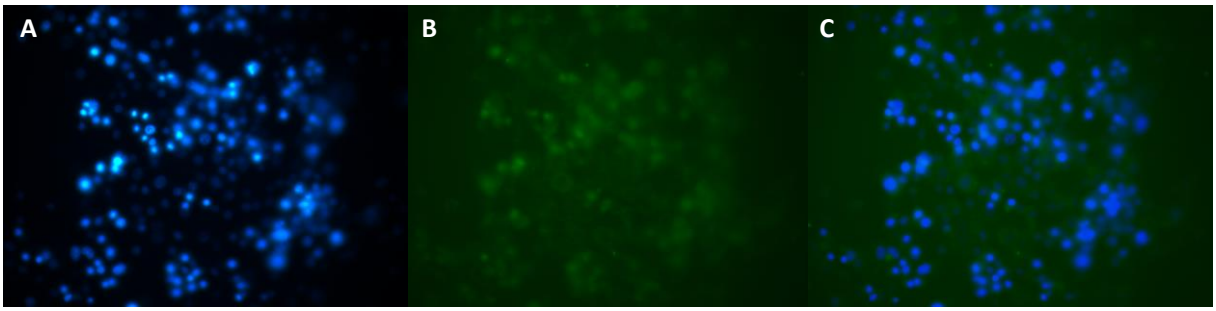

Figure 4.20. Fluorescence micrographs of NIH3T3 cells after incubation with Oregon Green (OG) labeled P(MAA-co-CMA) with 2 % CMA (Mw: 60 kDa) at 40X magnification a)Nucleus staining by DAPI b) Incubation with OG-labeled Copolymer c) Merge of a and b.

According to fluorescence microscope images, the copolymer was uptaken by NIH3T3 cells and distributed into cytosol, suggesting the escape from endosome/lysosome membrane. Despite the fact that this copolymer did not show membrane-lytic activity, the fluorescent labeled copolymer appeared to diffuse into cytosol. This result might be due to lower concentration of copolymer used in cell

culture studies (50 μM), supporting the discussion made in the previous section. Overall the results strongly suggest further investigations on the parameters affecting membrane-activity of P(MAA-co-CMA) and optimization of both copolymer composition, molecular weight and solution concentration to provide the best endosome-escaping ability.

CHAPTER 5

CONCLUSIONS

The aim of this thesis is to synthesize pH-sensitive, cholesterol containing polymers via reversible addition-fragmentation chain transfer (RAFT) polymerization as potential membrane-destabilizing agents for intracellular drug delivery applications and investigate interaction of these polymers with cell membrane. Cholesteryl methacrylate and 2-((Tert-butoxycarbony)(2-((tert-butoxycarbonyl) amino) ethyl) amino)ethyl methacrylate were synthesized. Cholesteryl methacrylate and t-butyl methacrylate random copolymers were synthesized at different molecular weights (4 – 60 kDa) and compositions (2, 4, 8 and 10 mol%). Copolymers were characterized using ^{1}H-NMR spectroscopy and gel permeation chromatography (GPC). Linear increase in ln $[M]_0/[M]$ with polymerization time, and Mn with monomer conversion indicated the RAFT-controlled copolymerization under the conditions tested. These synthesized copolymers were hydrolyzed to cholesteryl methacrylate-co-methacrylic acid copolymers as water soluble, pH-sensitive polyanions. The copolymers with 10 mol% CMA were not water-soluble even after hydrolysis, regardless of molecular weight. The pH-responsive behavior of copolymers was demonstrated via UV−visible spectroscopy and dynamic light scattering measurements. Both DLS measurements and hemolytic activity results indicated that the presence of cholesterol units along the copolymer chain enables the interactions with cell membrane, regardless the amount of cholesterol units, i.e. the presence of a few cholesterol units is sufficient to provide membrane-activity. However, the intrachain and interchain interactions between cholestrol units, depending on the copolymer concentration in solution, molecular weight of copolymer chains and pH of solution, strongly reduce membrane activity. The cell viability results (MTT assay) indicated that these copolymers at 250 μM concentration are not cytotoxic to NIH3T3 cell line.

Cholesteryl methacrylate was also copolymerized with 2-((tert-butoxycarbony)(2-((tert-butoxycarbonyl) amino) ethyl) amino)ethyl methacrylate to yield cholesterol containing polycations. The amine-protected copolymers with varying

CMA contents (10, 20 and 40 mol %) were synthesized. Copolymers were characterized using ^{1}H-NMR spectroscopy and GPC. Linear increase in ln $[M]_0/[M]$ with polymerization time, and Mn with monomer conversion indicated the RAFT-controlled copolymerization under the conditions tested. Increasing CMA content resulted in the deviation from linearity in kinetic plots, suggesting the partial loss of RAFT-controlled polymerization mechanism. The amine groups of copolymers were deprotected to have cationic copolymers. It was found that the copolymer having 40 mol% CMA was not water-soluble even after deprotection.

The following investigations can be the focus of future studies:

1. The molecular weight and solution concentration of P(MAA-co-CMA) copolymers can be further optimized to provide the best hemolytic activity. Accordingly lower molecular weight copolymers with 2 and 8 mol% CMA content can be synthesized and their hydrodynamic diameters and hemolytic activities can be tested at varying concentrations.

2. Cytotoxicity of AEAEMA-co-CMA copolymers with varying CMA content can be performed to determine whether these copolymers possess potential for drug delivery applications

3. Intracellular distribution and cellular uptake mechanisms of both types of copolymers can be investigated using florescent labelled polymers, organelle-specific fluorophores such endosome and lysosome-specific fluorophores, and endocytosis inhibitors.

REFERENCES

Abdullah, S., et al. (2010). "Gene transfer into the lung by nanoparticle dextran-spermine/plasmid DNA complexes." BioMed Research International **2010**.

Almeida, H., et al. (2012). "Temperature and pH stimuli-responsive polymers and their applications in controlled and selfregulated drug delivery." Journal of Applied Pharmaceutical Science **2**(6).

Alves, P., et al. (2013). "Effect of cholesterol-poly (N, N-dimethylaminoethyl methacrylate) on the properties of stimuli-responsive polymer liposome complexes." Colloids and Surfaces B: Biointerfaces **104**: 254-261.

Baker, A., et al. (1997). "Polyethylenimine (PEI) is a simple, inexpensive and effective reagent for condensing and linking plasmid DNA to adenovirus for gene delivery." Gene therapy **4**(8).

Behr, J.-P., et al. (1989). "Efficient gene transfer into mammalian primary endocrine cells with lipopolyamine-coated DNA." Proceedings of the National Academy of Sciences **86**(18): 6982-6986.

Berg, K., et al. (1999). "Photochemical internalization a novel technology for delivery of macromolecules into cytosol." Cancer Research **59**(6): 1180-1183.

Boussif, O., et al. (1995). "A versatile vector for gene and oligonucleotide transfer into cells in culture and in vivo: polyethylenimine." Proceedings of the National Academy of Sciences **92**(16): 7297-7301.

Broeckling, C. D., et al. (2008). "Root exudates regulate soil fungal community composition and diversity." Applied and Environmental Microbiology **74**(3): 738-744.

Bulmus, V., et al. (2003). "A new pH-responsive and glutathione-reactive, endosomal membrane-disruptive polymeric carrier for intracellular delivery of biomolecular drugs." Journal of Controlled Release **93**(2): 105-120.

Canton, I. and G. Battaglia (2012). "Endocytosis at the nanoscale." Chemical Society Reviews **41**(7): 2718-2739.

Caracciolo, G., et al. (2009). "Efficient escape from endosomes determines the superior efficiency of multicomponent lipoplexes." The Journal of Physical Chemistry B **113**(15): 4995-4997.

Chen, S., et al. (2010). "Enhanced gene transfection with addition of a cell-penetrating peptide in substrate-mediated gene delivery." The journal of gene medicine **12**(8): 705-713.

Du, Z., et al. (2012). "Polymerized spermine as a novel polycationic nucleic acid carrier system." International journal of pharmaceutics **434**(1): 437-443.

Duarte, S., et al. (2012). "Folate-associated lipoplexes mediate efficient gene delivery and potent antitumoral activity in vitro and in vivo." International journal of pharmaceutics **423**(2): 365-377.

Duncan, R. and S. C. Richardson (2012). "Endocytosis and intracellular trafficking as gateways for nanomedicine delivery: opportunities and challenges." Molecular pharmaceutics **9**(9): 2380-2402.

Felgner, P. L., et al. (1987). "Lipofection: a highly efficient, lipid-mediated DNA-transfection procedure." Proceedings of the National Academy of Sciences **84**(21): 7413-7417.

Filion, M. C. and N. C. Phillips (1997). "Toxicity and immunomodulatory activity of liposomal vectors formulated with cationic lipids toward immune effector cells." Biochimica et Biophysica Acta (BBA)-Biomembranes **1329**(2): 345-356.

Gao, X. and L. Huang (1991). "A novel cationic liposome reagent for efficient transfection of mammalian cells." Biochemical and biophysical research communications **179**(1): 280-285.

Godbey, W., et al. (1999). "Size matters: molecular weight affects the efficiency of poly (ethyleneimine) as a gene delivery vehicle." Journal of biomedical materials research **45**(3): 268-275.

Greber, U. F., et al. (1994). "Mechanisms of virus uncoating." Trends in microbiology **2**(2): 52-56.

Han, J. and Y. Il Yeom (2000). "Specific gene transfer mediated by galactosylated poly-L-lysine into hepatoma cells." International journal of pharmaceutics **202**(1): 151-160.

Harrison, S. C. (1995). "Virus structures and conformational rearrangements." Current opinion in structural biology **5**(2): 157-164.

Henry, S. M., et al. (2006). "pH-responsive poly (styrene-alt-maleic anhydride) alkylamide copolymers for intracellular drug delivery." Biomacromolecules **7**(8): 2407-2414.

Joanne, P., et al. (2009). "Antimicrobial peptides and viral fusion peptides: how different they are?" Protein and peptide letters **16**(7): 743-750.

Kiang, T., et al. (2004). "Formulation of chitosan-DNA nanoparticles with poly (propyl acrylic acid) enhances gene expression." Journal of Biomaterials Science, Polymer Edition **15**(11): 1405-1421.

Knipe, D. M., et al. (1996). "Virus-host cell interactions." Fields virology **1**: 273-299.

Kurosaki, T., et al. (2009). "Exploitation of De Novo helper-lipids for effective gene delivery." Journal of pharmacy & pharmaceutical sciences **11**(4): 56-67.

Kurtulus, I., et al. (2014). "A new proton sponge polymer synthesized by RAFT polymerization for intracellular delivery of biotherapeutics." Polymer Chemistry.

Kwon, E., et al. (2008). "Peptide-modified vectors for nucleic acid delivery to neurons." Journal of Controlled Release **132**(3): 230-235.

Kwon, E. J., et al. (2010). "A truncated HGP peptide sequence that retains endosomolytic activity and improves gene delivery efficiencies." Molecular pharmaceutics **7**(4): 1260-1265.

Leventis, R. and J. R. Silvius (1990). "Interactions of mammalian cells with lipid dispersions containing novel metabolizable cationic amphiphiles." Biochimica et Biophysica Acta (BBA)-Biomembranes **1023**(1): 124-132.

Lollo, C., et al. (2000). "Obstacles and advances in non-viral gene delivery." Current opinion in molecular therapeutics **2**(2): 136.

Mangipudi, S. S., et al. (2009). "Development of a genetically engineered biomimetic vector for targeted gene transfer to breast cancer cells." Molecular pharmaceutics **6**(4): 1100-1109.

McCarthy, H. O., et al. (2011). "Evaluation of a multi-functional nanocarrier for targeted breast cancer iNOS gene therapy." International journal of pharmaceutics **405**(1): 196-202.

McCrudden, C. M. and H. O. McCarthy (2013). "Cancer Gene Therapy–Key Biological Concepts in the Design of Multifunctional Non-Viral Delivery Systems."

Merkel, O. M., et al. (2011). "Pulmonary gene delivery using polymeric nonviral vectors." Bioconjugate chemistry **23**(1): 3-20.

Meunier-Durmort, C., et al. (1997). "Adenovirus enhancement of polyethylenimine-mediated transfer of regulated genes in differentiated cells." Gene therapy **4**(8).

Michael, S. and D. Curiel (1994). "Strategies to achieve targeted gene delivery via the receptor-mediated endocytosis pathway." Gene therapy **1**(4): 223-232.

Mudhakir, D. and H. Harashima (2009). "Learning from the viral journey: how to enter cells and how to overcome intracellular barriers to reach the nucleus." The AAPS journal **11**(1): 65-77.

Murthy, N., et al. (1999). "The design and synthesis of polymers for eukaryotic membrane disruption." Journal of Controlled Release **61**(1): 137-143.

Panariti, A., et al. (2012). "The effect of nanoparticle uptake on cellular behavior: disrupting or enabling functions?" Nanotechnology, science and applications **5**: 87.

Sevimli, S., et al. (2012). "Well-defined cholesterol polymers with pH-controlled membrane switching activity." Biomacromolecules **13**(10): 3064-3075.

Sevimli, S., et al. (2012). "Synthesis, self-assembly and stimuli responsive properties of cholesterol conjugated polymers." Polymer Chemistry **3**(8): 2057-2069.

Shenk, T. E. (1996). Adenoviridae: the viruses and their replication.

Soldati, T. and M. Schliwa (2006). "Powering membrane traffic in endocytosis and recycling." Nature Reviews Molecular Cell Biology **7**(12): 897-908.

Sternberg, B., et al. (1998). "Ultrastructural characterization of cationic liposome-DNA complexes showing enhanced stability in serum and high transfection activity in vivo." Biochimica et Biophysica Acta (BBA)-Biomembranes **1375**(1): 23-35.

Tonge, S. and B. Tighe (2001). "Responsive hydrophobically associating polymers: a review of structure and properties." Advanced drug delivery reviews **53**(1): 109-122.

Torchilin, V. P. (2008). "Cell penetrating peptide-modified pharmaceutical nanocarriers for intracellular drug and gene delivery." Peptide Science **90**(5): 604-610.

Tweten, R. K. (2005). "Cholesterol-dependent cytolysins, a family of versatile pore-forming toxins." Infection and immunity **73**(10): 6199-6209.

Wadia, J. S., et al. (2004). "Transducible TAT-HA fusogenic peptide enhances escape of TAT-fusion proteins after lipid raft macropinocytosis." Nature medicine **10**(3): 310-315.

Wagner, E., et al. (1992). "Influenza virus hemagglutinin HA-2 N-terminal fusogenic peptides augment gene transfer by transferrin-polylysine-DNA complexes: toward a synthetic virus-like gene-transfer vehicle." Proceedings of the National Academy of Sciences **89**(17): 7934-7938.

Wang, Y., et al. (2014). "pH-sensitive pullulan-based nanoparticles for intracellular drug delivery." Polymer Chemistry **5**(2): 423-432.

White, J. M. (1992). "Membrane fusion." Science **258**(5084): 917-924.

Wolfrum, C., et al. (2007). "Mechanisms and optimization of in vivo delivery of lipophilic siRNAs." Nature biotechnology **25**(10): 1149-1157.

Wyman, T. B., et al. (1997). "Design, synthesis, and characterization of a cationic peptide that binds to nucleic acids and permeabilizes bilayers." Biochemistry **36**(10): 3008-3017.

APPENDIX A

^{1}H-NMR OF COPOLYMERIZATION OF P(T-BMA-CO-CMA)

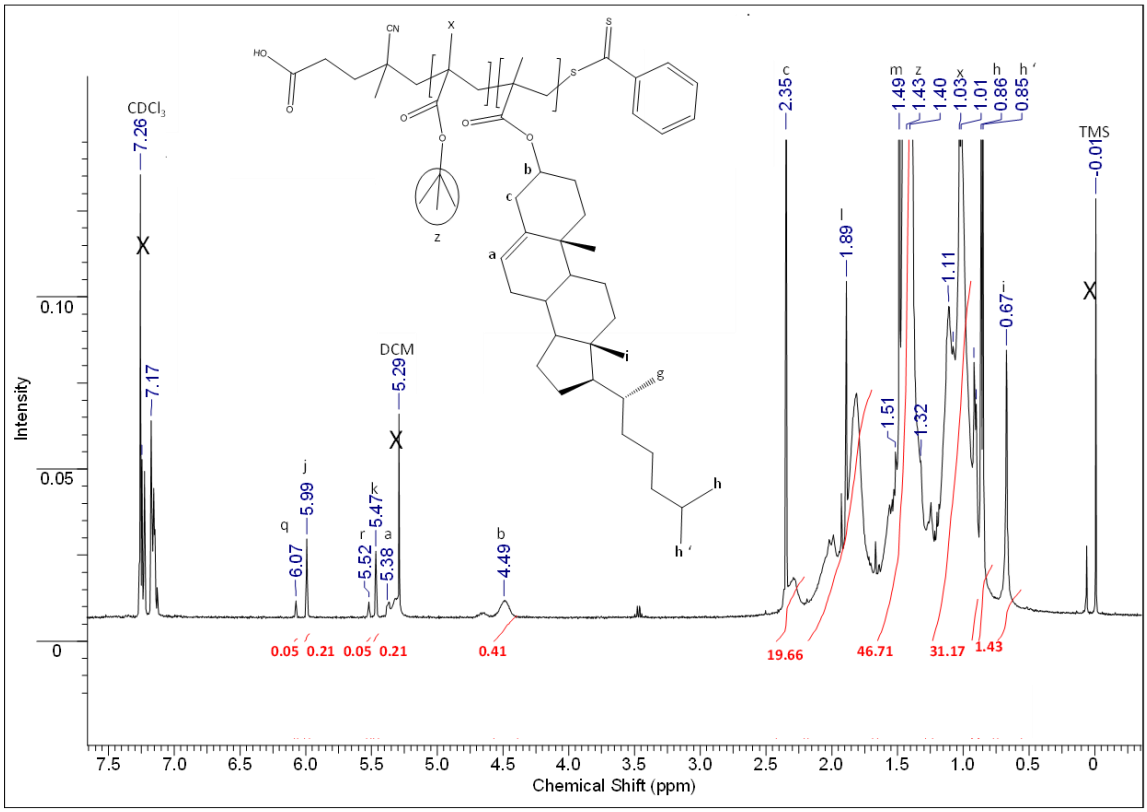

Figure A.1. Representative ^{1}H-NMR spectra of copolymerization mixture of cholesteryl methacrylate and tert-butyl methacrylate [Total Monomer]= 4.2 M; [t-BMA]/[CMA]/[RAFT]/[AIBN] mole ratio= 450/50/1/0.2; Mn = 89517 g/mol; CMA= 10.4%).

APPENDIX B

^{1}H-NMR OF COPOLYMERIZATION P(BOC-AEAEMA-CO-CMA)

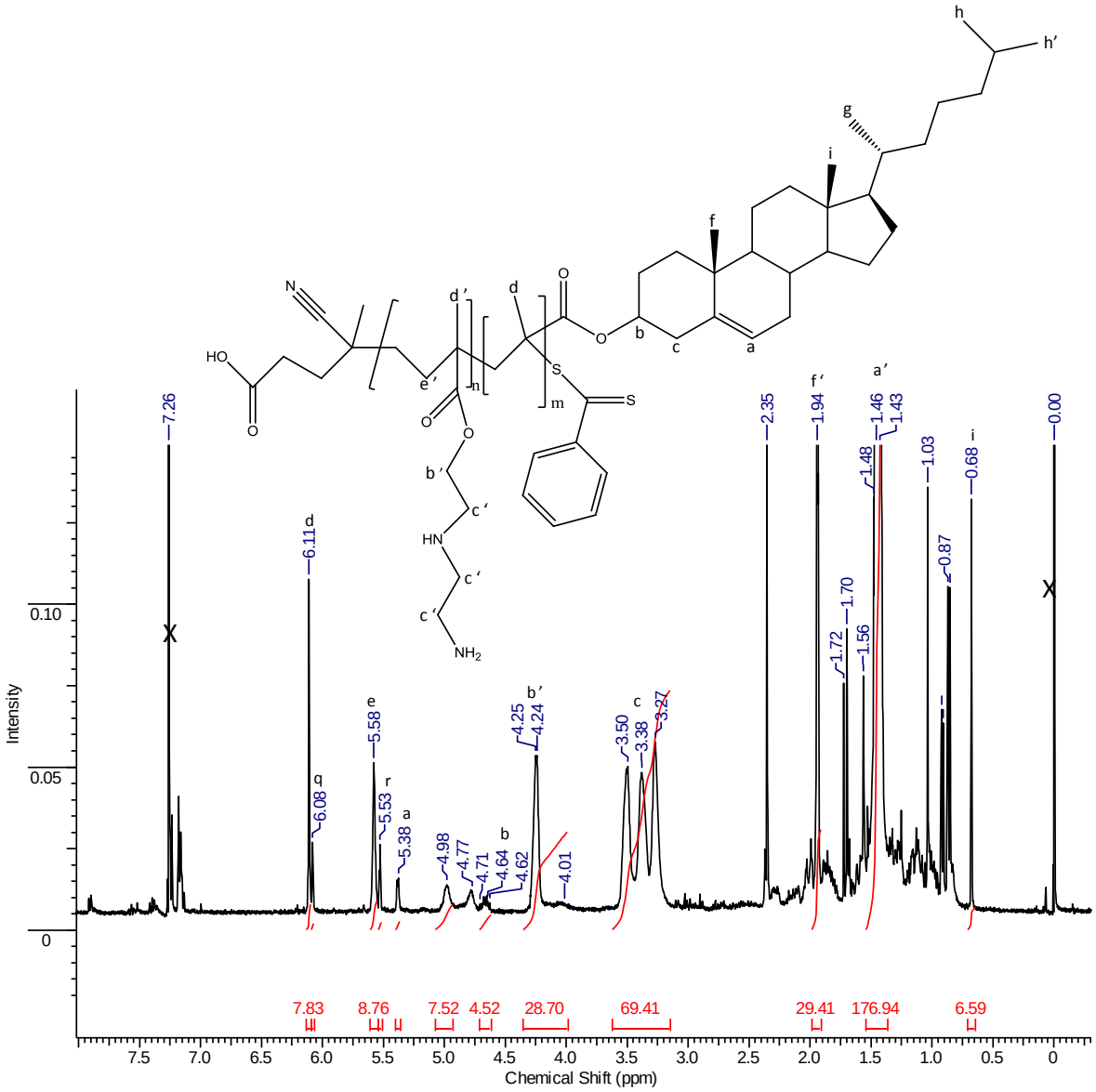

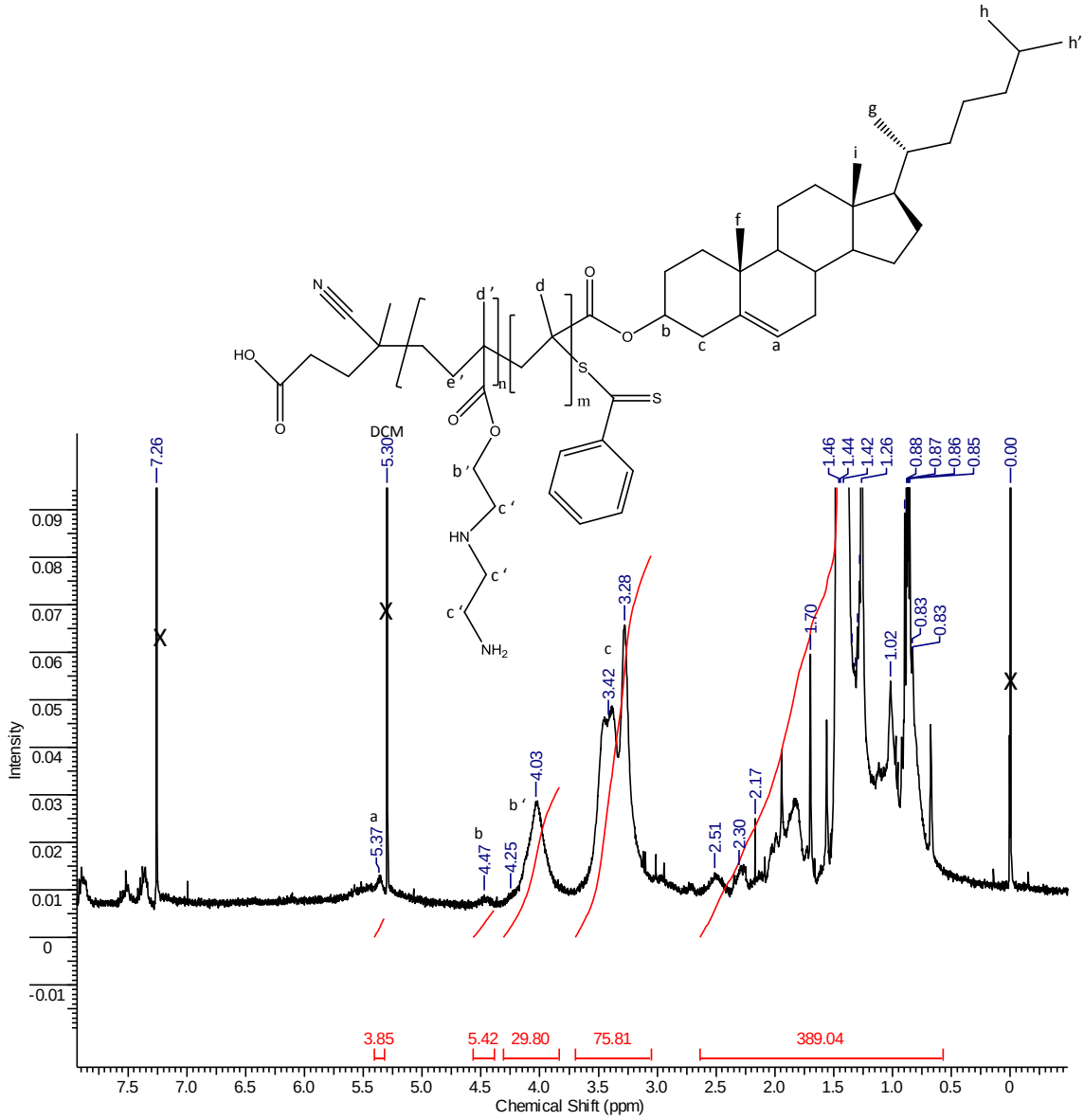

Figure A2. Representative ^{1}H-NMR spectra of copolymerization mixture of cholesteryl methacrylate and 2-((tert-butoxycarbony) (2-((tert-butoxycarbonyl) amino) ethyl) amino) ethyl methacrylate and purified p(CMA-co-Boc-AEAEMA) (bottom). ([Total Monomer] = 1.5 M; [Boc-AEAEMA]/[CMA]/[RAFT]/[AIBN]= 22.5/2.5/1/0.25).

APPENDIX C

GPC CHROMATOGRAMS OF P(T-BMA-CO-CMA)

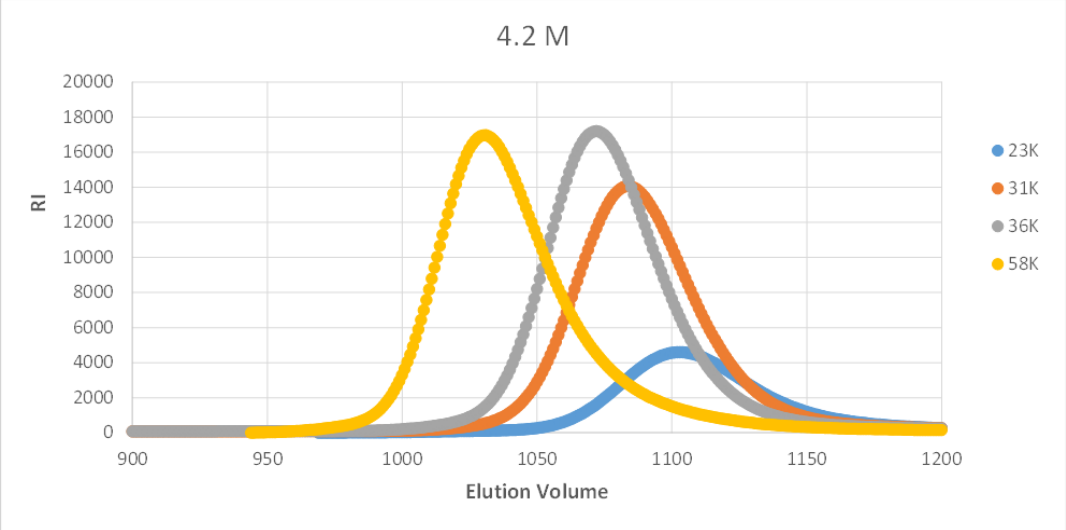

Figure C.1. GPC chromatograms of copolymerization mixture when monomer concentration was 4.2 M and [M]/[R]/[I] ratios was 500/1/0.25.

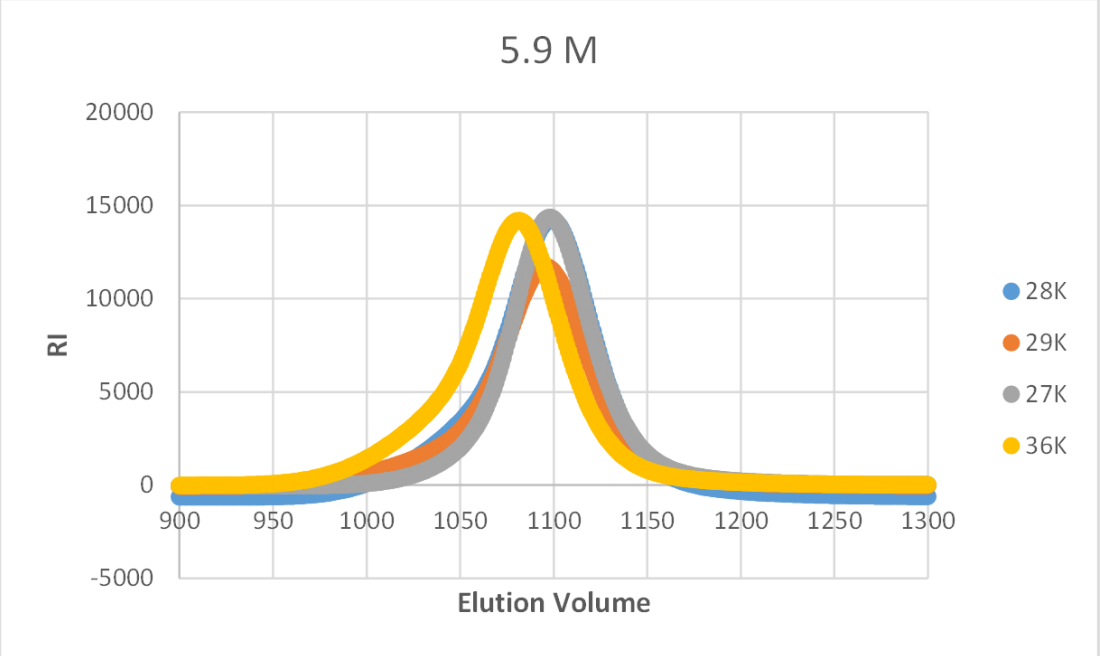

Figure C.2. GPC chromatograms of copolymerization mixture when monomer concentration was 5.9 M and [M]/[R]/[I] ratios was 500/1/0.25.